Dissimilar Catalytic Behavior of Molecular or Colloidal Palladium Systems with a New NHC Ligand

Fernando Gómez-Villarraga[a,1], Jonathan De Tovar[a,1], Miguel Guerrero[b,c], Pau Nolis[d], Teodor Parella,[d] Pierre Lecante,[e] Nuria Romero[a], Lluís Escriche[a], Roger Bofill[a], Josep Ros[a], Xavier Sala[a], Karine Philippot[b,c]*, and Jordi García-Antón[a]*.

[a] Dr. F. Gómez-Villarraga, J. De Tovar, Dr. N. Romero, Dr. L. Escriche, Dr. R. Bofill Dr. J. Ros, Dr. X. Sala, Dr. J. García-Antón
Departament de Química, Unitat de Química Inorgànica, Universitat Autònoma de Barcelona, 08193-Bellaterra, Barcelona, Spain.
Fax: (+34) 93 581 3101
*E-mail: Jordi.GarciaAnton@uab.es

[b] Dr. M. Guerrero, Dr. K. Philippot
CNRS; LCC (Laboratoire de Chimie de Coordination du CNRS), 205, route de Narbonne, F-31077 Toulouse, France
Fax: (+33) 5 61553003
*E-mail: Karine.Philippot@lcc-toulouse.fr

[c] Université de Toulouse; UPS, INPT ; LCC ; F-31077 Toulouse, France

[d] Servei de Ressonància Magnètica Nuclear (SeRMN), Universitat Autònoma de Barcelona, E-08193, Bellaterra, Spain

[e] CNRS, CEMES (Centre d'Elaboration de Matériaux et d'Etudes Structurales), 29 rue J. Marvig, F-31055 Toulouse, France

[1] These authors equally contributed to this work.

Supplementary information

Supplementary Information

Tables:

Figures:

Figure S14. Infrared spectrum of **C1**.

Figure S15. 1D and 2D NMR spectra (360 MHz, 298K, dmso-d_6) for **C2**: (a) ^{1}H-NMR, (b) ^{13}C{^{1}H}-NMR, (c) HSQC NMR, (d) COSY NMR.

Figure S16. ESI-MS spectrum of **C2**.

Figure S17. Infrared spectrum of **C2**.

Figure S18. HR-TEM micrographs of Pd nanoparticles (a) **N1** and (b) **N2** after catalytic experiments.

Table S1. Crystallographic data for **C2**.

	C2
Molecular Formula	$C_{18}H_{23}Cl_3N_4Pd$
Formula weigh	508.15
Temperature (K)	180(2)
Wavelength (Å)	0.71073
System, space group	Orthorhombic, P 21 21 21
Unit cell dimensions	
a (Å)	11.9601(3)
b (Å)	12.4291(3)
c (Å)	13.7982(3)
α (º)	90
β (º)	90
γ (º)	90
U (Å ^{3})	2051.15(8)
Z	4
D_{calc} (g cm^{-3})	1.646
μ (mm^{-1})	1.305
F(000)	1024
Crystal size (mm^3)	0.18x0.08x0.02
hkl ranges	-16<=h<=14, -17<=k<=16, -17<=l<=16
2 θ Range (º)	3.35 to 25.35
Reflections collected / unique / [R_{int}]	31319 / 5805 / [R(int) = 0.0302]
Completeness to θ (θ = 30.10º)	97.5 %
Absorption correction	Semi-empirical
Data/restrains/parameters	5805 / 0 / 238
Goodness-of-fit on F^2	1.016
Final R indices [I>2 σ (I)]	R1 = 0.0239, wR2 = 0.0467
R indices (all data)	R1 = 0.0308, wR2 = 0.0492
Largest diff. peak and hole (e Å^{-3})	0.887 and -0.303

Table S2. Selected bond lengths (Å) and bond angles (deg) for **C2**.

C2	
Pd – N(1)	2.0293(14)
Pd – Cl(1)	2.3102(6)
Pd – Cl(2)	2.2969(5)
Pd – Cl(3)	2.2991(5)
N(1) – Pd – Cl(1)	88.15(5)
N(1) – Pd– Cl(2)	179.24(6)
N(1) – Pd – Cl(3)	90.44(4)
Cl(1) – Pd– Cl(2)	91.816(19)
Cl(1) – Pd – Cl(3)	178.46(2)
Cl(2) – Pd– Cl(3)	89.587(19)

Figure S1. 1D and 2D NMR spectra (360 MHz, 298K, $CDCl_3$) for 1-[2-(3,5-dimethylpyrazol-1-yl)ethyl]-3-((S)-1-phenylethyl)-3H-imidazol-1-ium chloride (**HLCl**): (a) ^{1}H-NMR, (b) $^{13}C\{^{1}H\}$-NMR, (c) HSQC NMR, (d) COSY NMR.

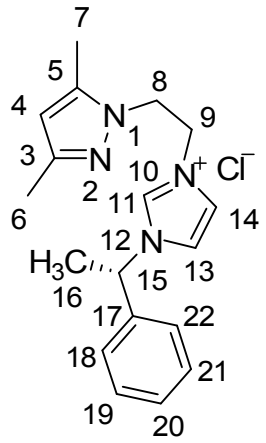

(a)

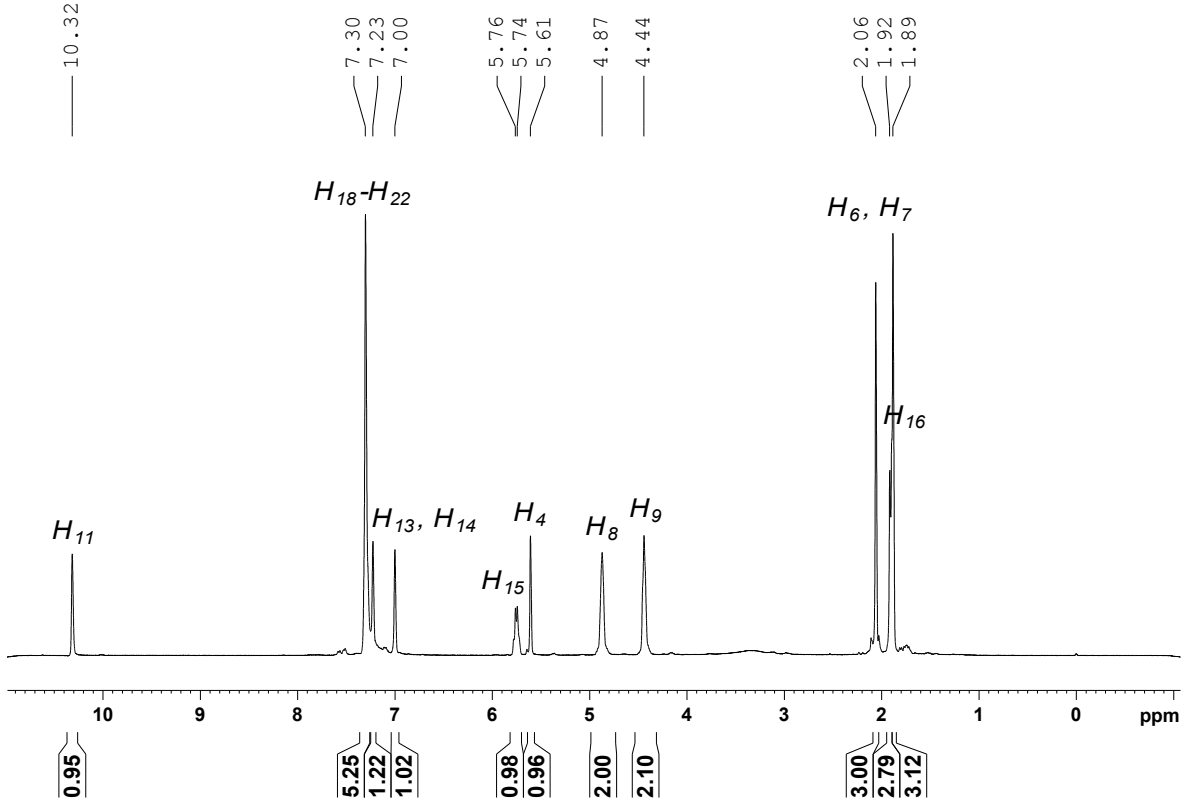

(b)

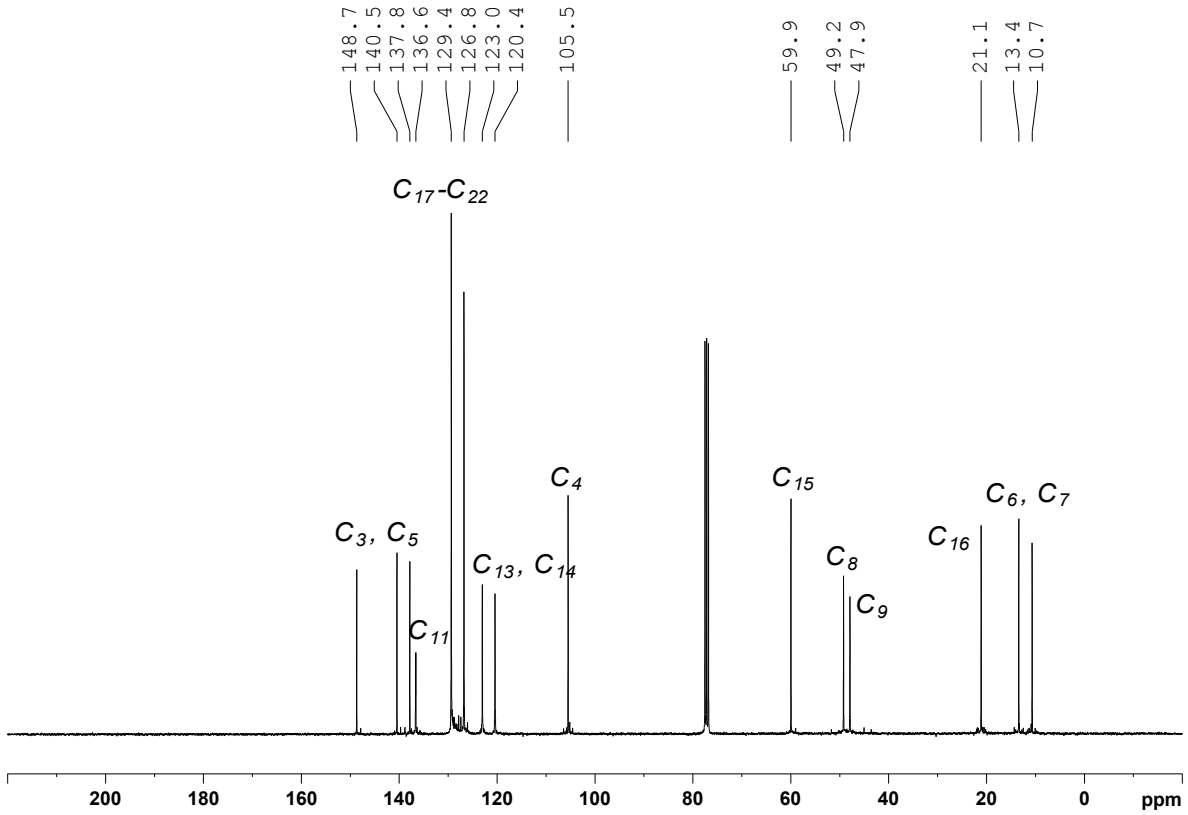
148.7
140.5
137.8
136.6
129.4
126.8
123.0
120.4
105.5
59.9
49.2
47.9
21.1
13.4
10.7
C17-C22
C3, C5
C11
C13, C14
C4
C15
C8
C9
C16
C6, C7
200
180
160
140
120
100
80
60
40
20
0
ppm

(c)

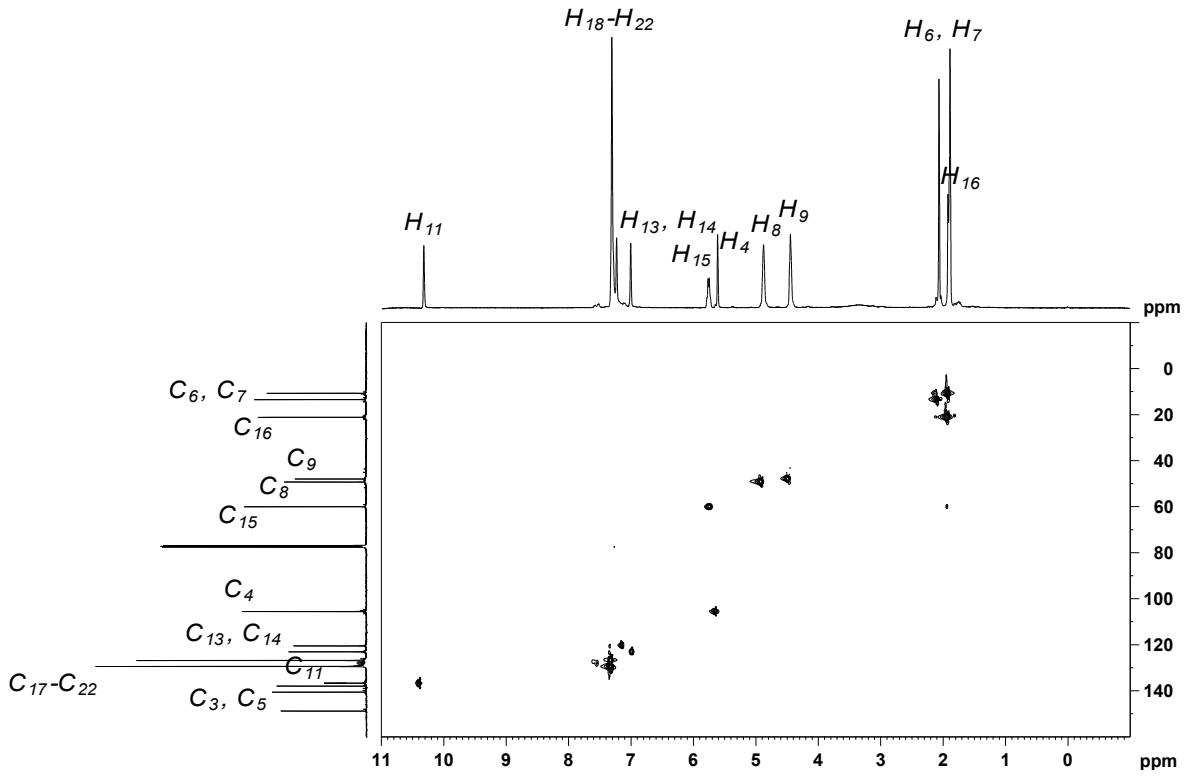
H18-H22
H6, H7
H16
H11
H13, H14
H15
H4
H8
H9
ppm
C6, C7
C16
C9
C8
C15
C4
C13, C14
C11
C17-C22
C3, C5
0
20
40
60
80
100
120
140
11
10
9
8
7
6
5
4
3
2
1
0
ppm

(d)

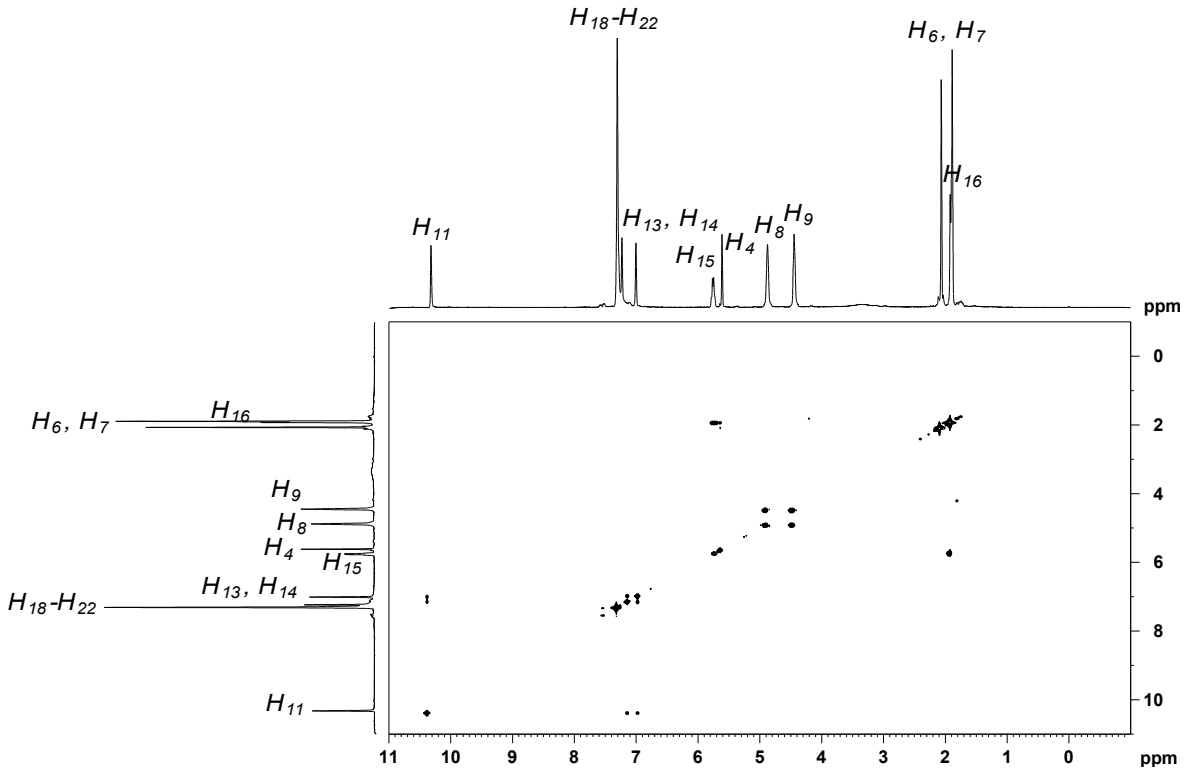
H18-H22
H6, H7
H16
H11
H13, H14
H15
H4
H8
H9
ppm
0
2
4
6
8
10
11
10
9
8
7
6
5
4
3
2
1
0
ppm

Figure S2. 1D and 2D NMR spectra (360 MHz, 298K, dmso-d_6) for 1-[2-(3,5-dimethylpyrazol-1-yl)ethyl]-3-((S)-1-phenylethyl)-3H-imidazol-1-ium chloride (**HLCl**): (a) ^{1}H-NMR, (b) ^{13}C{^{1}H}-NMR, (c) HSQC NMR, (d) COSY NMR.

(a)

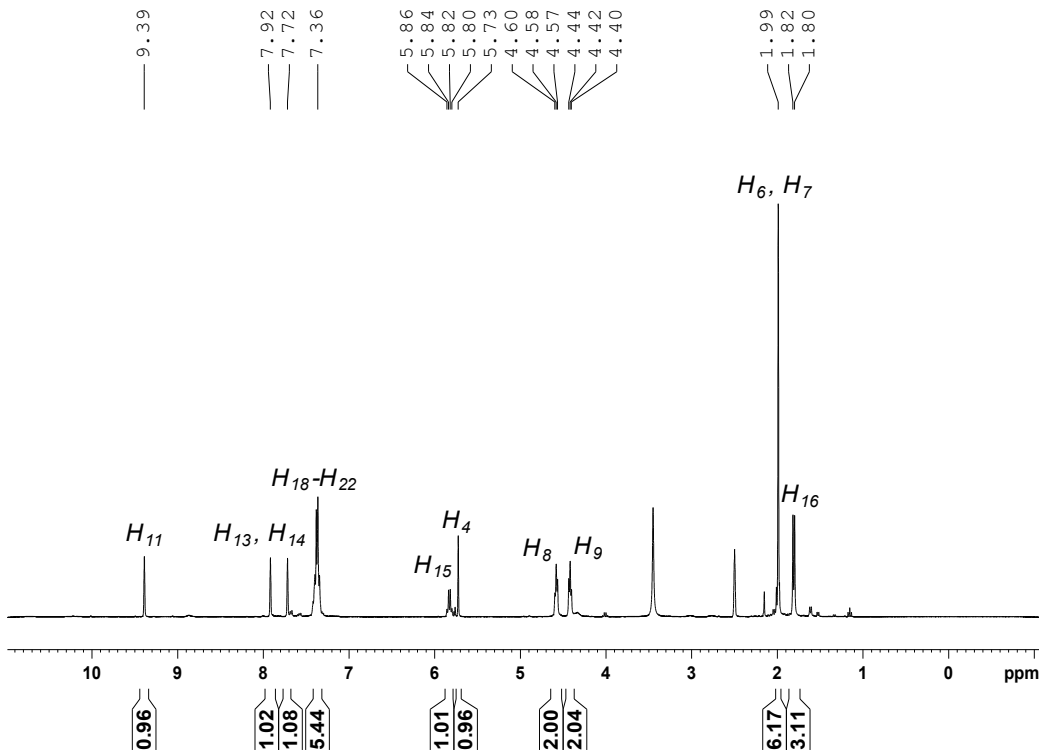

(b)

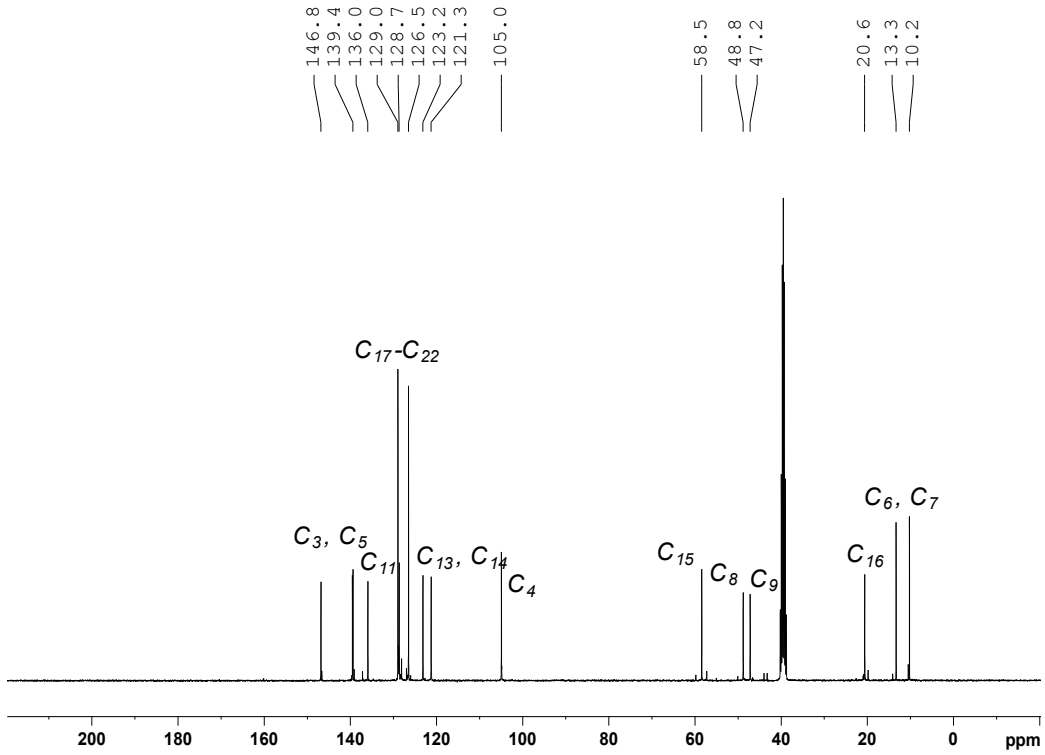

(c)

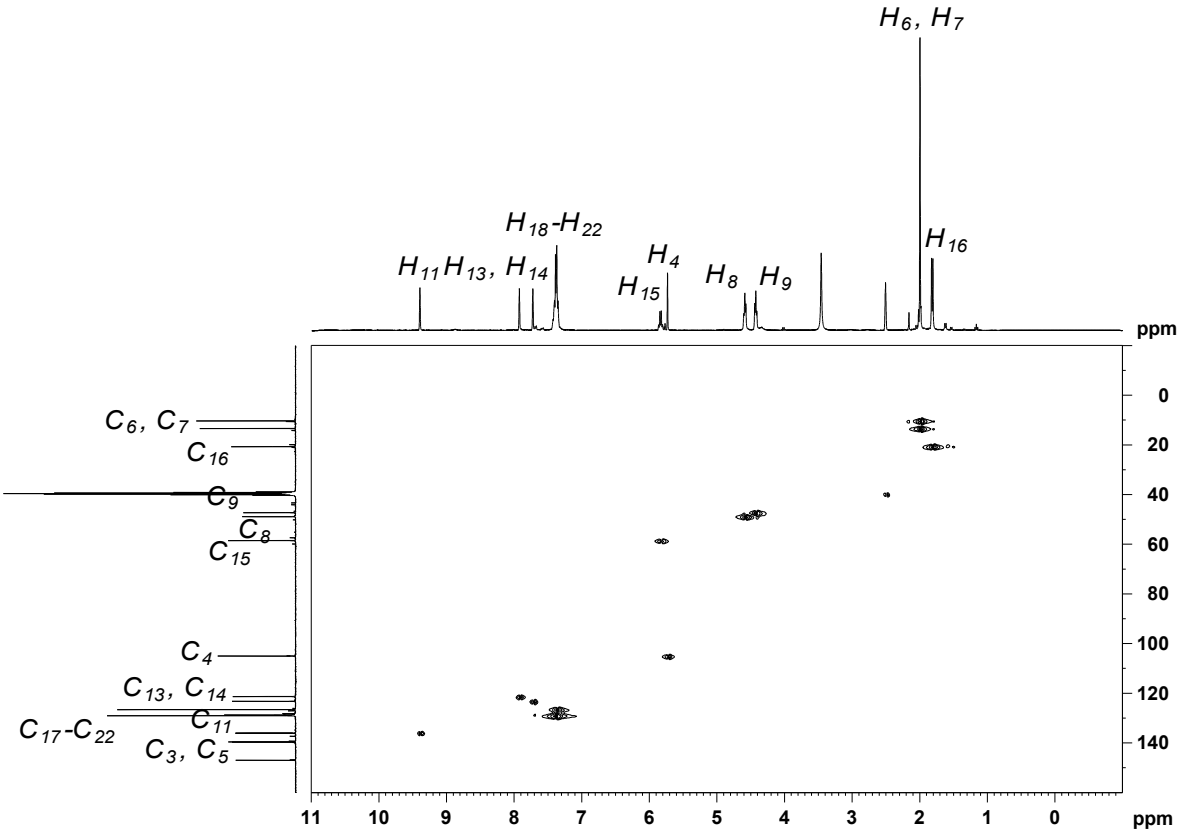
H6, H7
H18-H22
H11H13, H14
H4
H15
H8
H9
H16
ppm
C6, C7
C16
C9
C8
C15
C4
C13, C14
C11
C17-C22
C3, C5
11 10 9 8 7 6 5 4 3 2 1 0 ppm
0 20 40 60 80 100 120 140

(d)

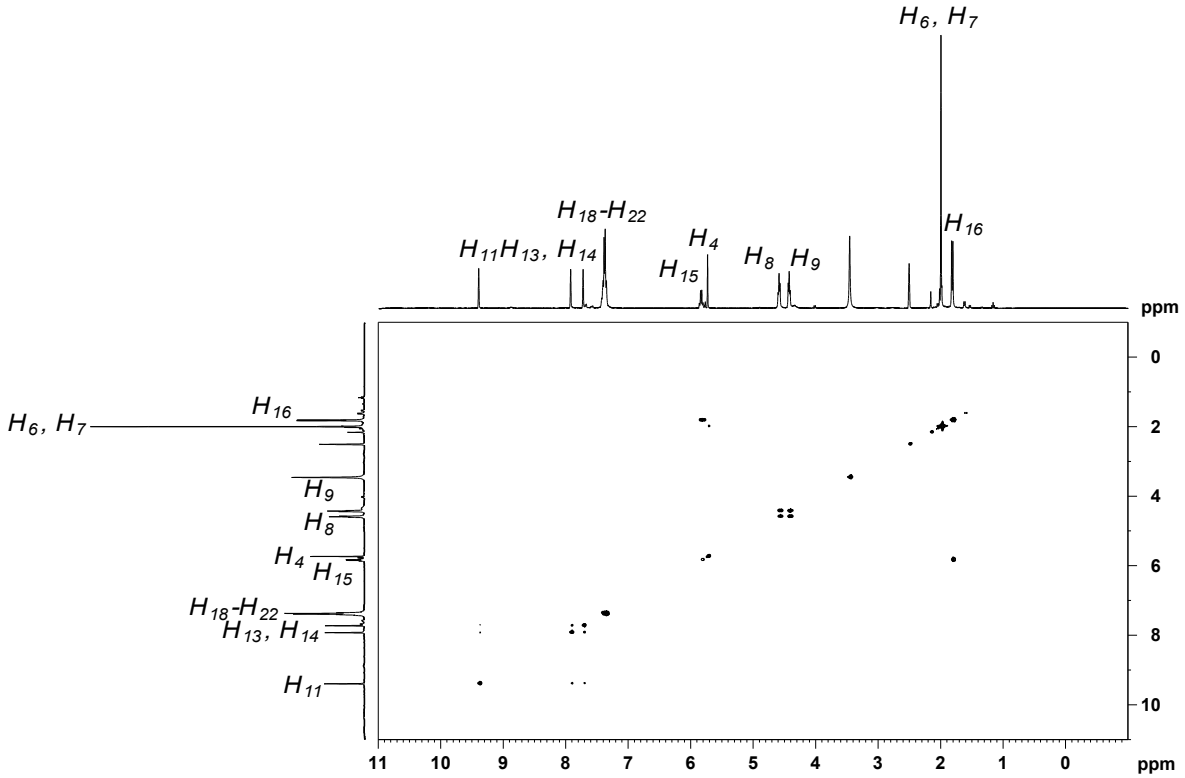
H6, H7
H18-H22
H11H13, H14
H4
H15
H8
H9
H16
ppm
H16
H6, H7
H9
H8
H4
H15
H18-H22
H13, H14
H11
11 10 9 8 7 6 5 4 3 2 1 0 ppm
0 2 4 6 8 10

Figure S3. ESI-MS spectrum of 1-[2-(3,5-dimethylpyrazol-1-yl)ethyl]-3-((S)-1-phenylethyl)-3H-imidazol-1-ium chloride (**HLCl**).

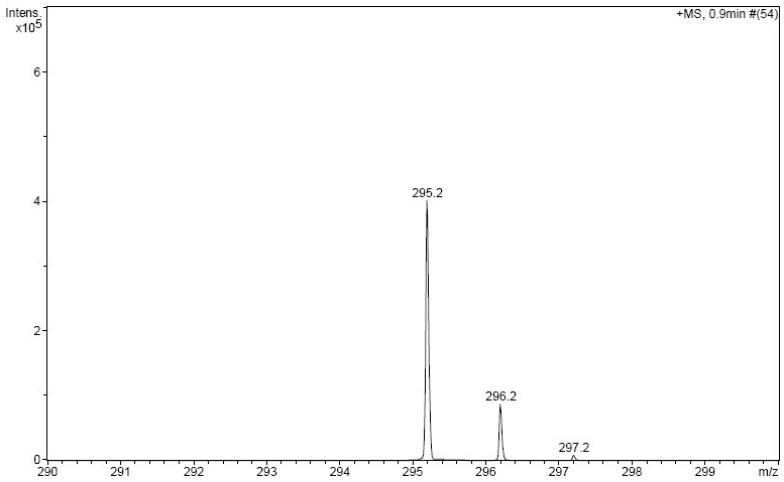

Figure S4. Infrared spectrum of 1-[2-(3,5-dimethylpyrazol-1-yl)ethyl]-3-((S)-1-phenylethyl)-3H-imidazol-1-ium chloride (**HLCl**).

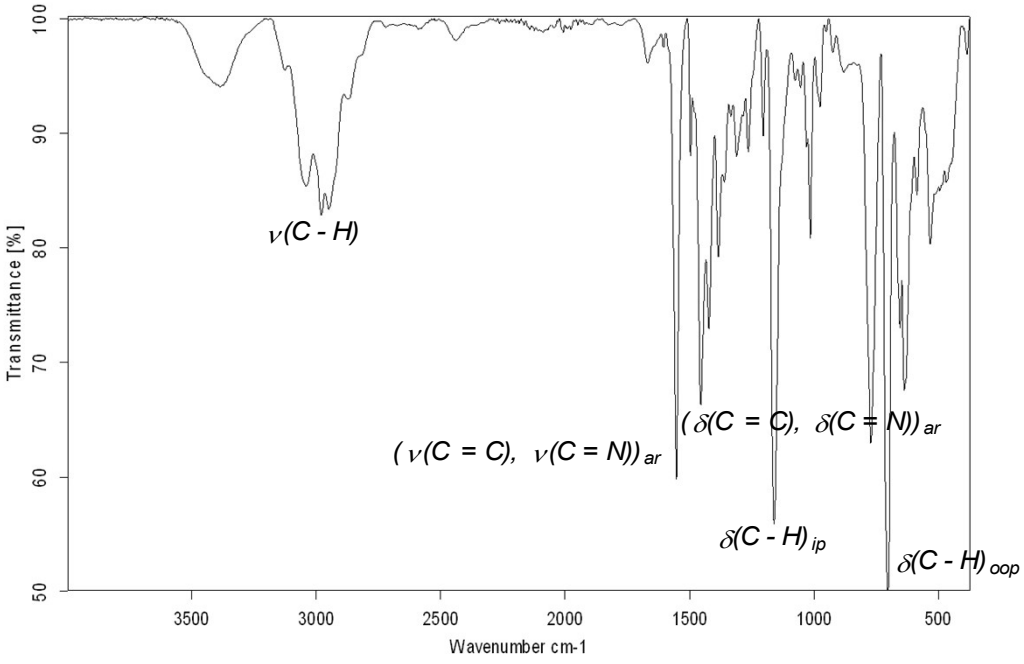

Figure S5. 1D and 2D NMR spectra (400 MHz, 298K, $CDCl_3$) for 1-[2-(3,5-dimethylpyrazol-1-yl)ethyl]-3-((S)-1-phenylethyl)-3H-imidazol-2-ylidene (**L**): (a) ^{1}H-NMR, (b) $^{13}C\{^{1}H\}$-NMR, (c) HSQC NMR, (d) COSY NMR.

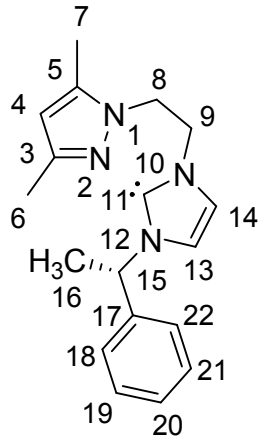

(a)

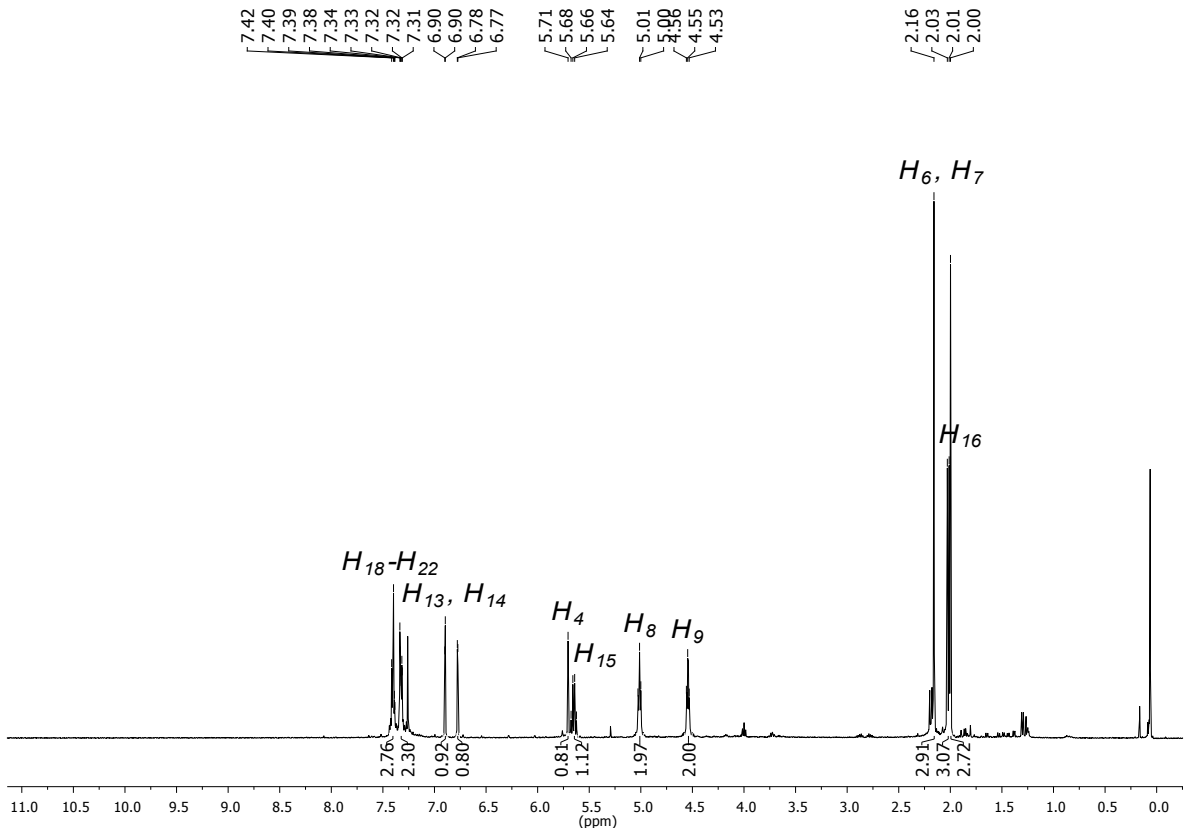

(b)

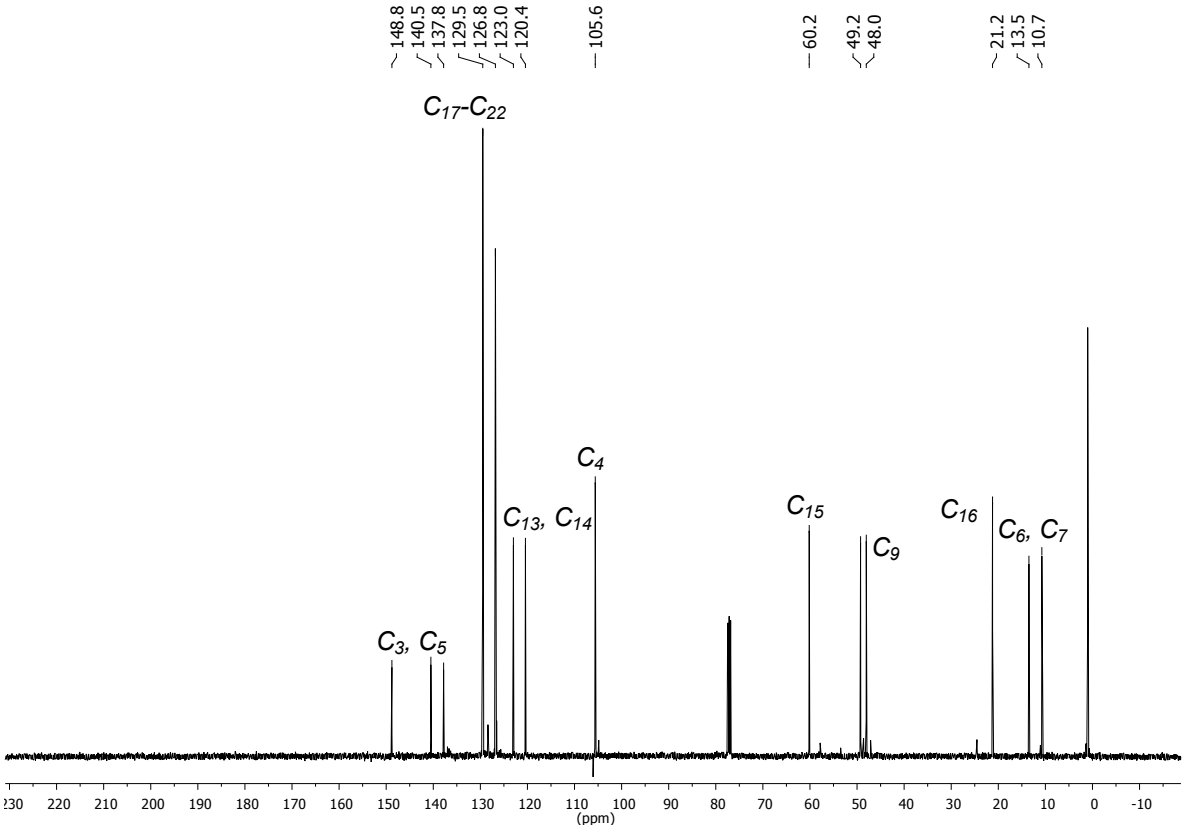
148.8
140.5
137.8
129.5
126.8
123.0
120.4
105.6
60.2
49.2
48.0
21.2
13.5
10.7
C17-C22
C4
C13, C14
C15
C16
C9
C6, C7
C3, C5
(ppm)

(c)

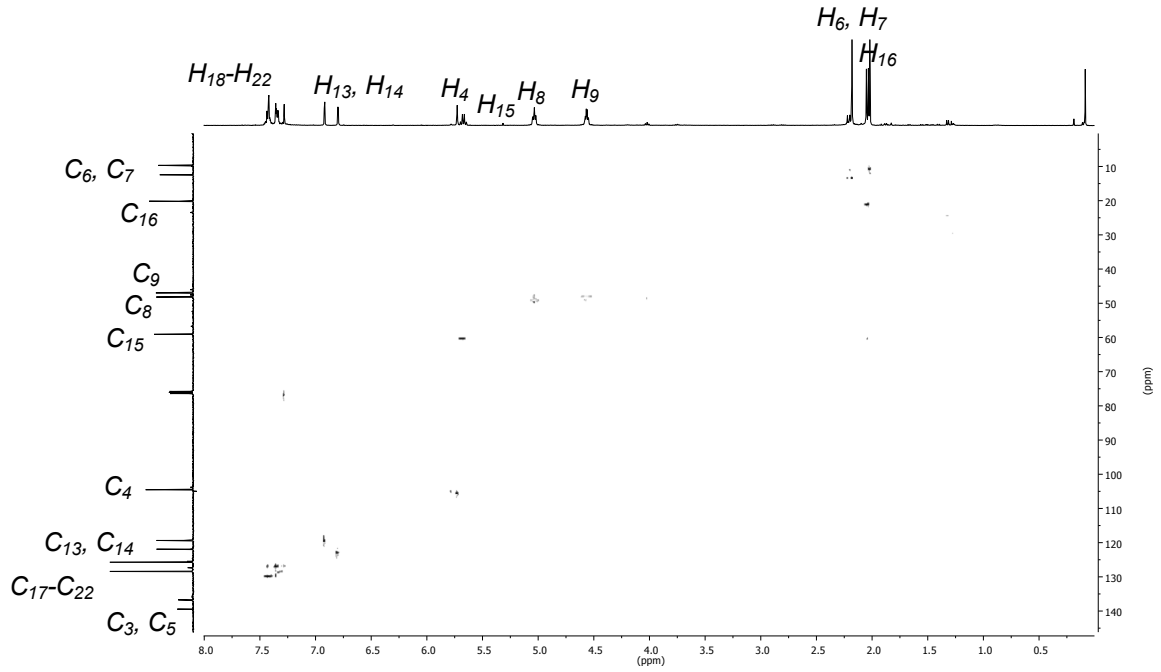
H6, H7
H16
H18-H22
H13, H14
H4
H15
H8
H9
C6, C7
C16
C9
C8
C15
C4
C13, C14
C17-C22
C3, C5
(ppm)
(ppm)

(d)

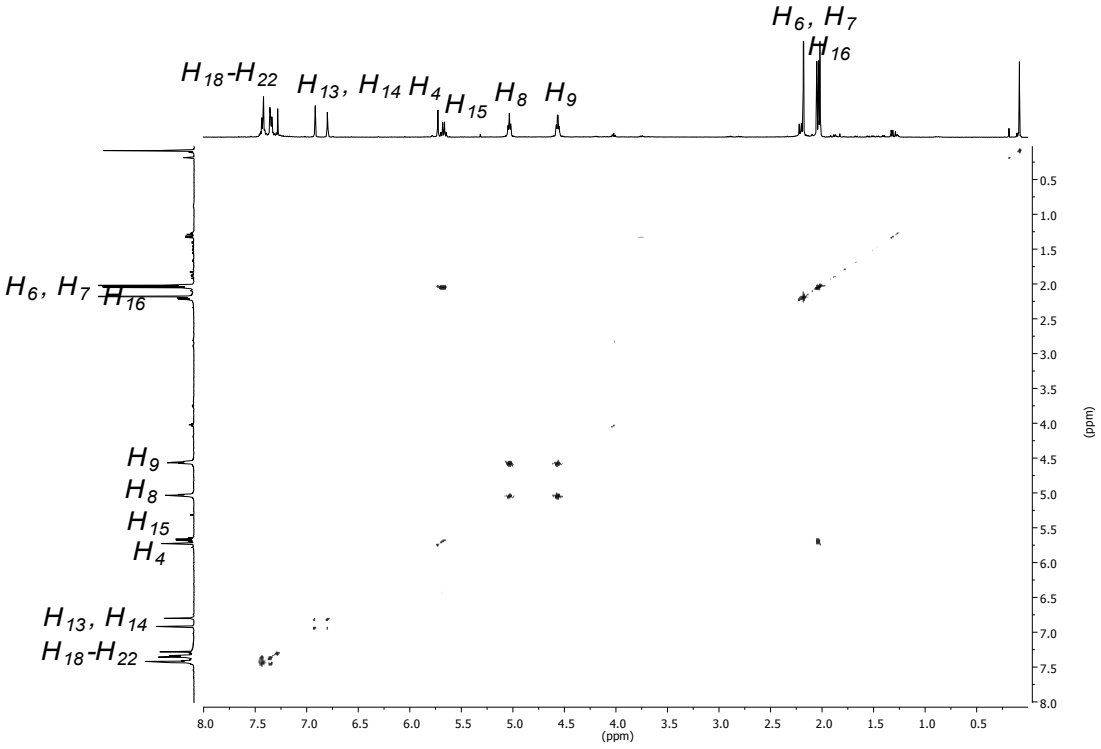

Figure S6. Infrared spectrum of 1-[2-(3,5-dimethylpyrazol-1-yl)ethyl]-3-((S)-1-phenylethyl)-3H-imidazol-2-ylidene (**L**).

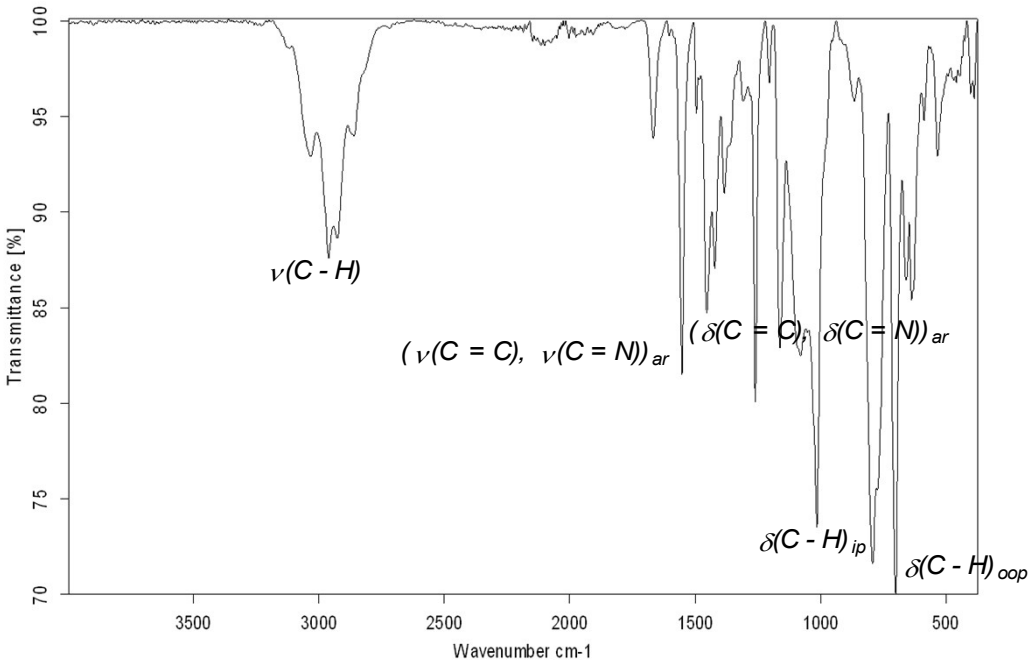

Figure S7. SEM-FEG analyses of the Pd materials produced with (a) [**L**]/[Pd] = 0.1; (b) [**HLCl**]/[Pd] = 0.3; (c) [**HLCl**]/[Pd] = 0.5; (d) [**HLCl**]/[Pd] = 1.0.

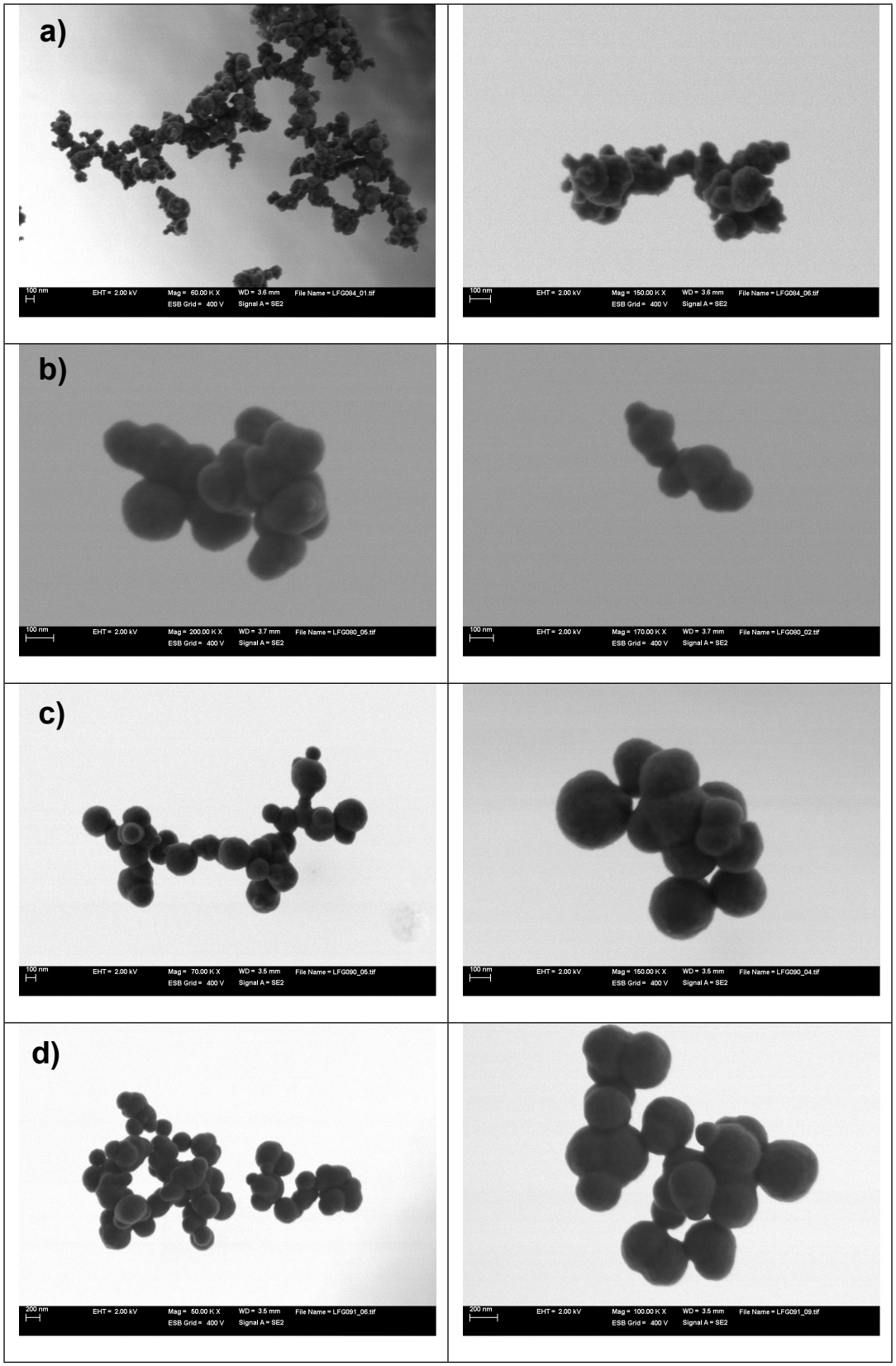

Figure S8. Infrared spectrum of (a) **N1** and (b) **N2**.

(a)

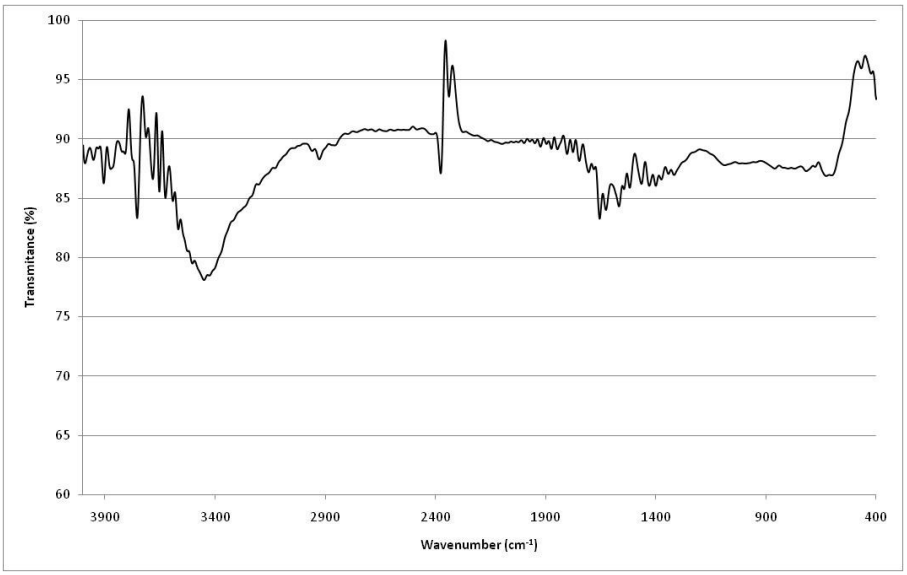

(b)

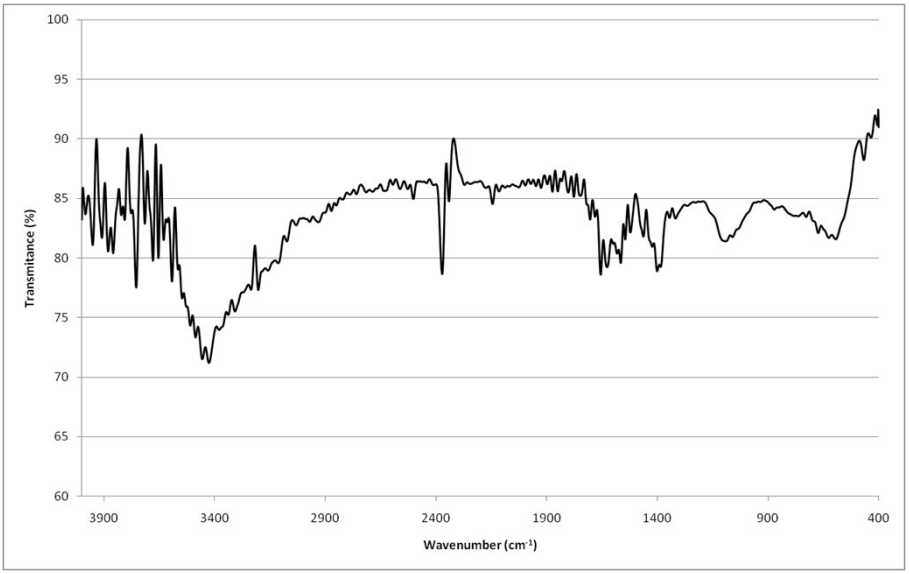

	L	N1	LHCl	N2
ν (C-H)	3033, 2960	3026, 2939	3040, 2978	3019, 2960
(ν (C=C), ν (C=N))ar	1552	1564	1552	1563
(δ(C=C), δ (C=N))ar	1454	1462	1455	1456
δ (C-H)ip	1015	-	1160	1137
δ (C-H)oop	700	700	703	-

Figure S9. 1D and 2D NMR spectra (360 MHz, 298K, $CDCl_3$) for Chloro[(*S*)-3-(2-(3,5-dimethyl-1*H*-pyrazol-1-yl)ethyl)-1-(1-phenylethyl)-1*H*-imidazol-2-ylidiene)]silver(I) **(C_{Ag})**: (a) ^{1}H-NMR, (b) $^{13}C\{^{1}H\}$-NMR, (c) HSQC NMR, (d) COSY NMR.

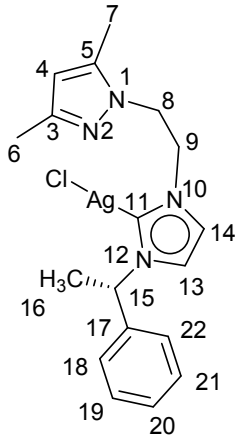

(a)

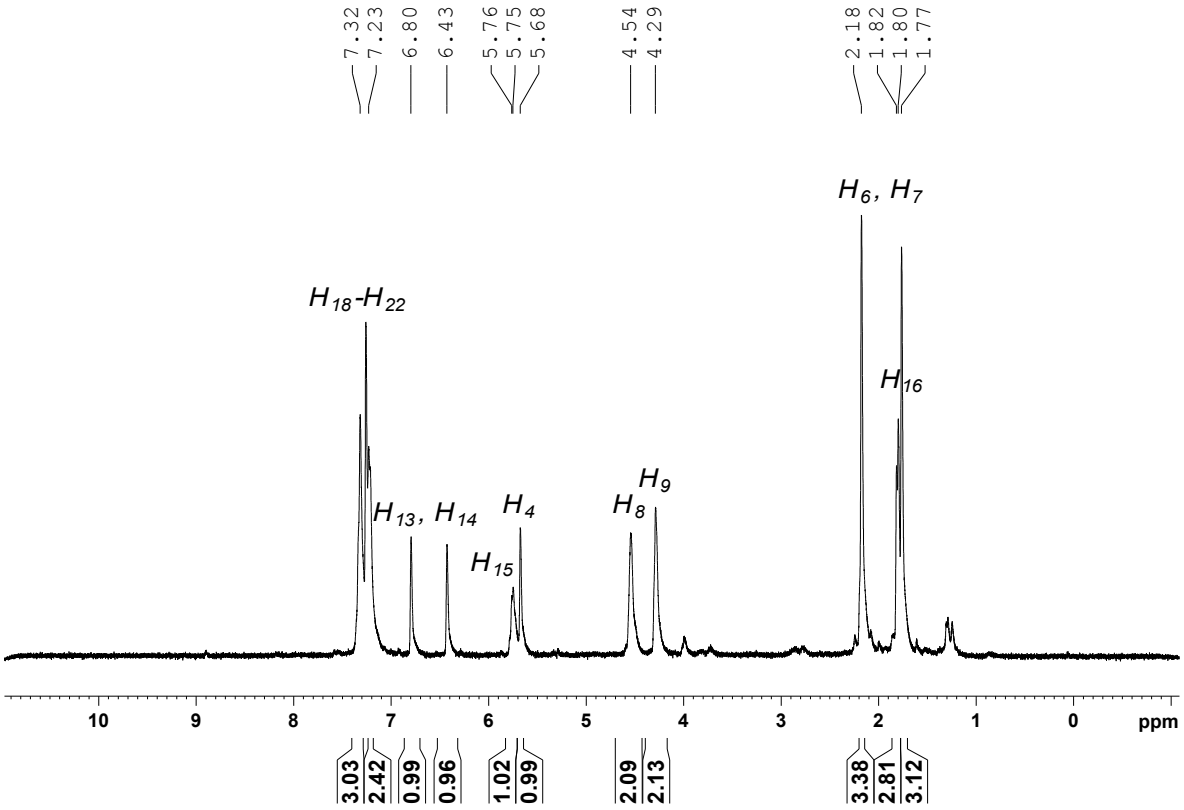

(b)

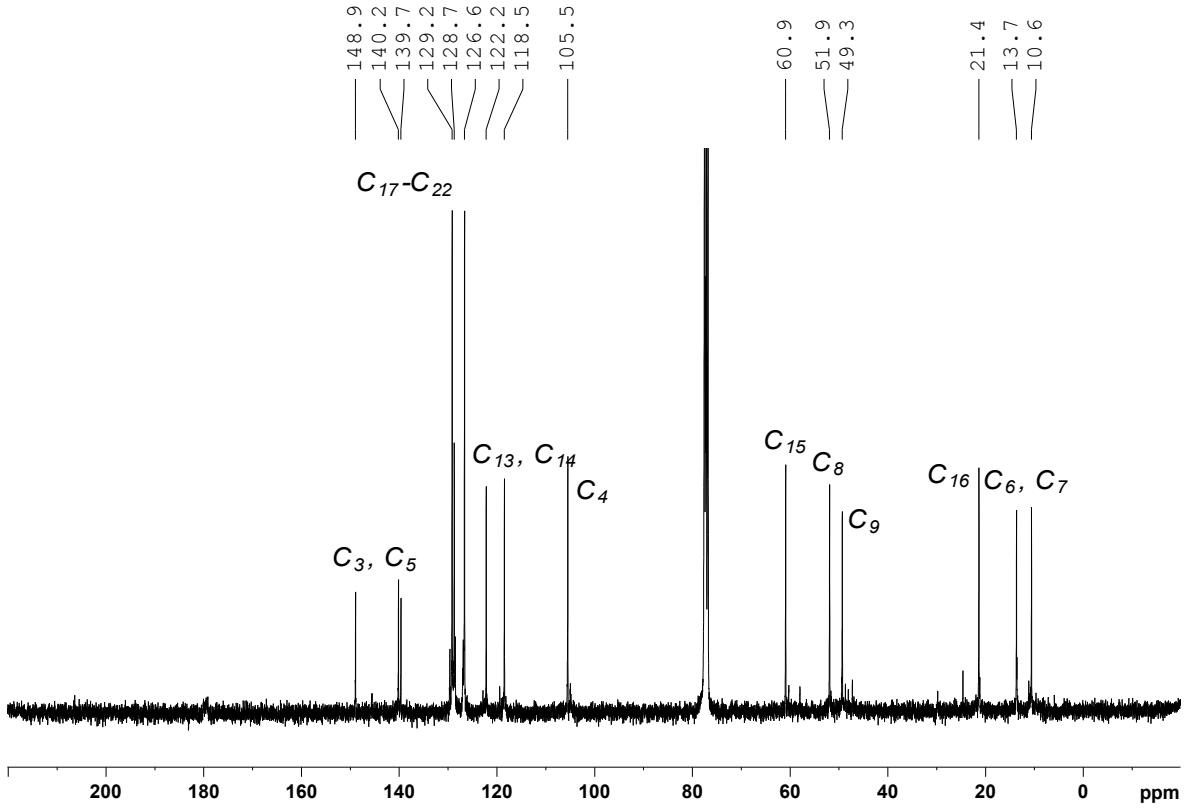
148.9
140.2
139.7
129.2
128.7
126.6
122.2
118.5
105.5
60.9
51.9
49.3
21.4
13.7
10.6
C17-C22
C13, C14
C4
C3, C5
C15
C8
C9
C16
C6, C7
200
180
160
140
120
100
80
60
40
20
0
ppm

(c)

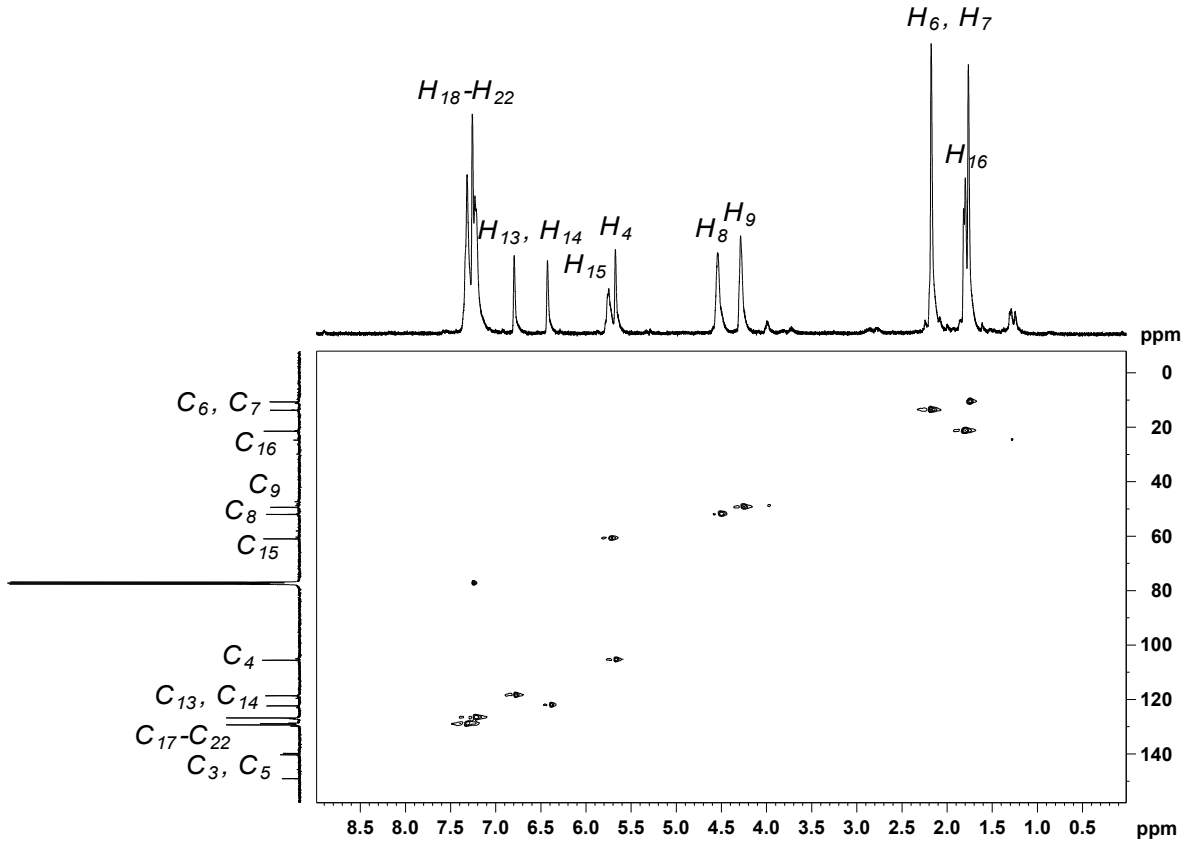
H6, H7
H18-H22
H16
H13, H14
H4
H15
H8
H9
ppm
C6, C7
C16
C9
C8
C15
C4
C13, C14
C17-C22
C3, C5
0
20
40
60
80
100
120
140
8.5 8.0 7.5 7.0 6.5 6.0 5.5 5.0 4.5 4.0 3.5 3.0 2.5 2.0 1.5 1.0 0.5
ppm

(d)

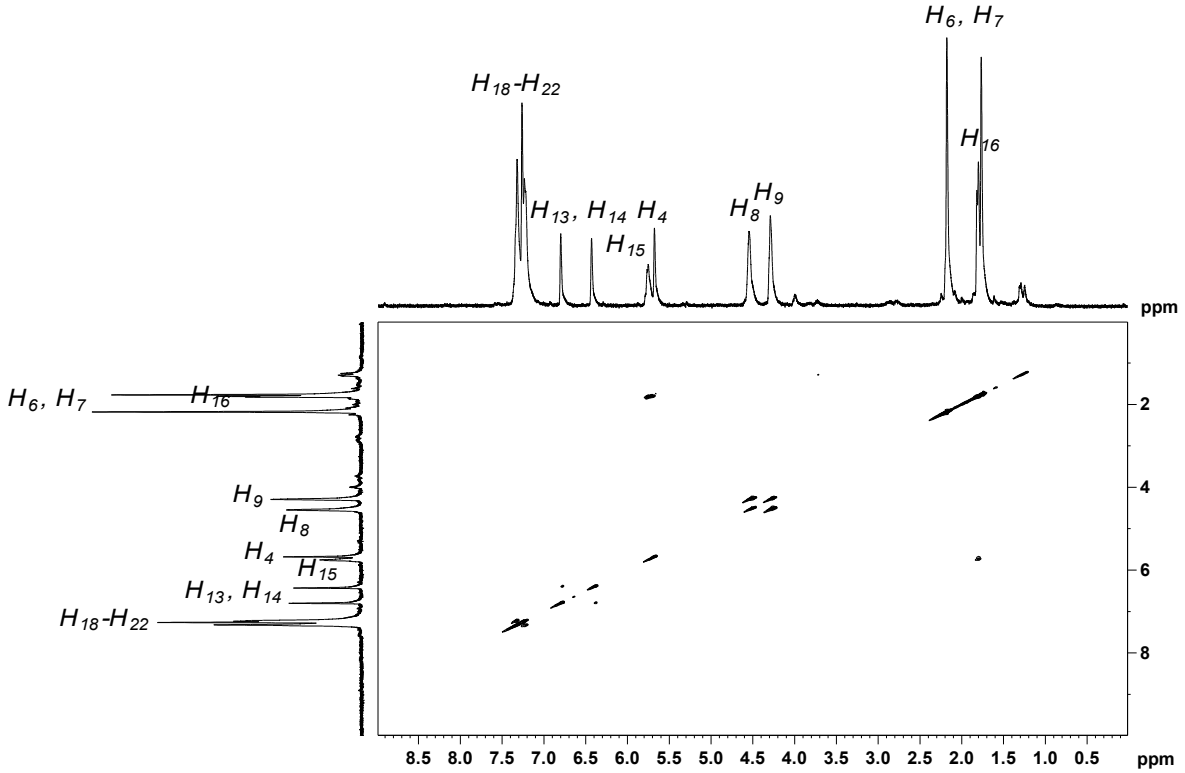
H6, H7
H18-H22
H16
H13, H14
H4
H15
H8
H9
ppm
H6, H7
H16
H9
H8
H4
H15
H13, H14
H18-H22
2
4
6
8
8.5 8.0 7.5 7.0 6.5 6.0 5.5 5.0 4.5 4.0 3.5 3.0 2.5 2.0 1.5 1.0 0.5
ppm

Figure S10. ESI-MS spectrum of $\mathbf{C_{Ag}}$.

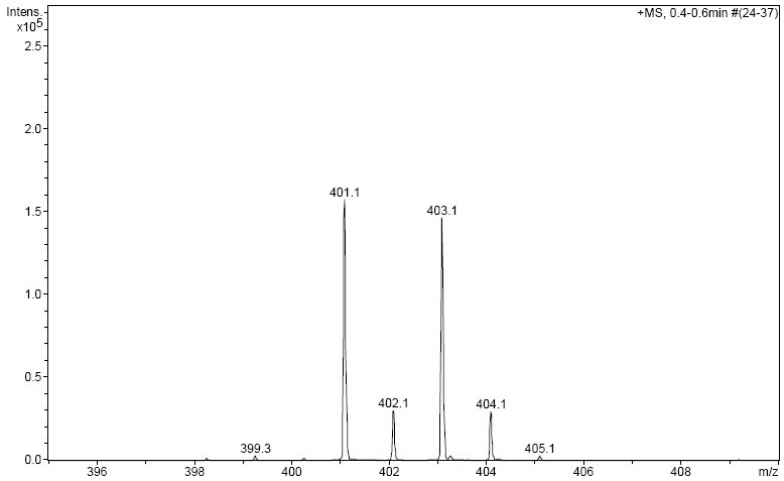

Figure S11. Infrared spectrum of $\mathbf{C_{Ag}}$.

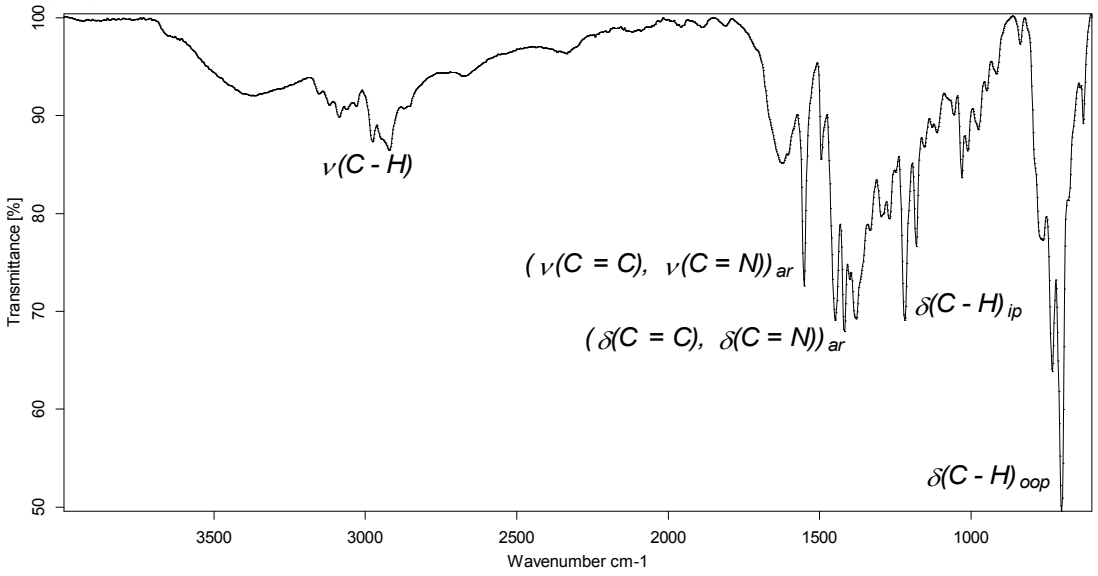

Figure S12. 1D and 2D NMR spectra (600 MHz, 298K, $CDCl_3$) for dichloro[(*S*)-3-(2-(3,5-dimethyl-1*H*-pyrazol-1-yl)ethyl)-1-(1-phenylethyl)-1*H*-imidazol-2-ylidiene)-κ^1*N*]palladium(II), (**C1**): (a) ^{1}H-NMR, (b) ^{13}C{^{1}H}-NMR, (c) COSY NMR, (d) ROESY NMR, (e) HSQC NMR, (f) HMBC NMR.

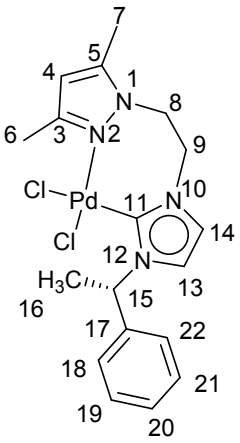

(a)

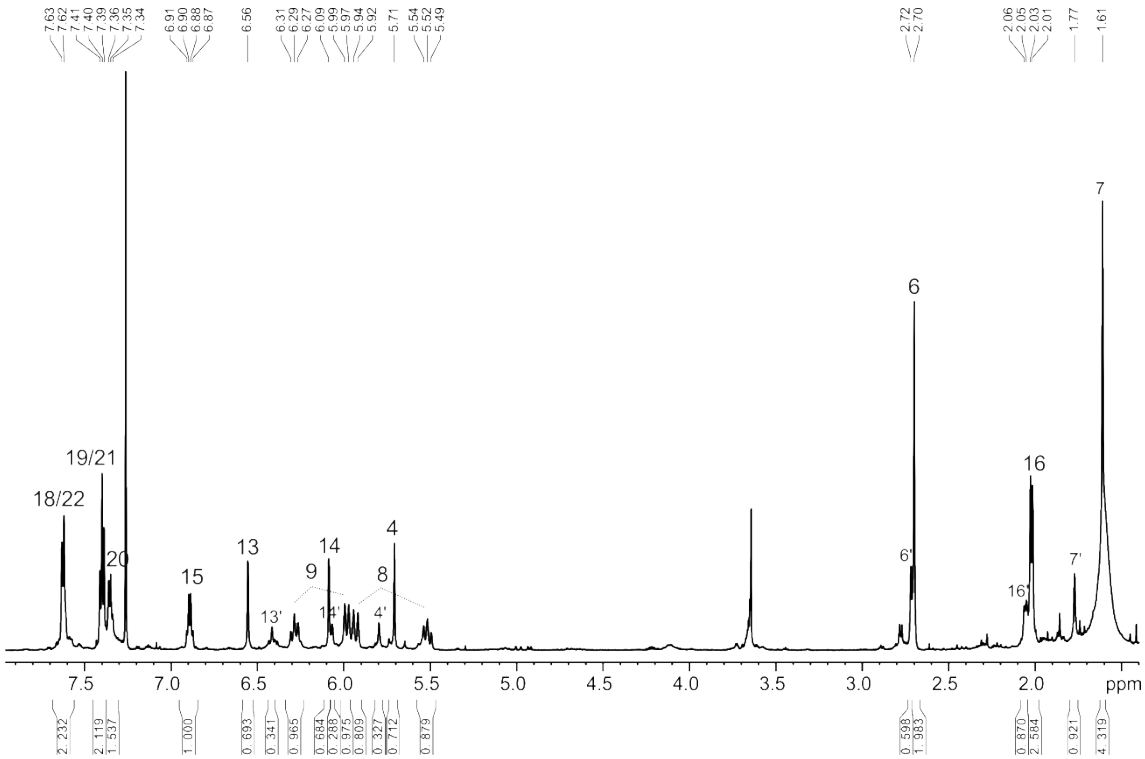

(b)

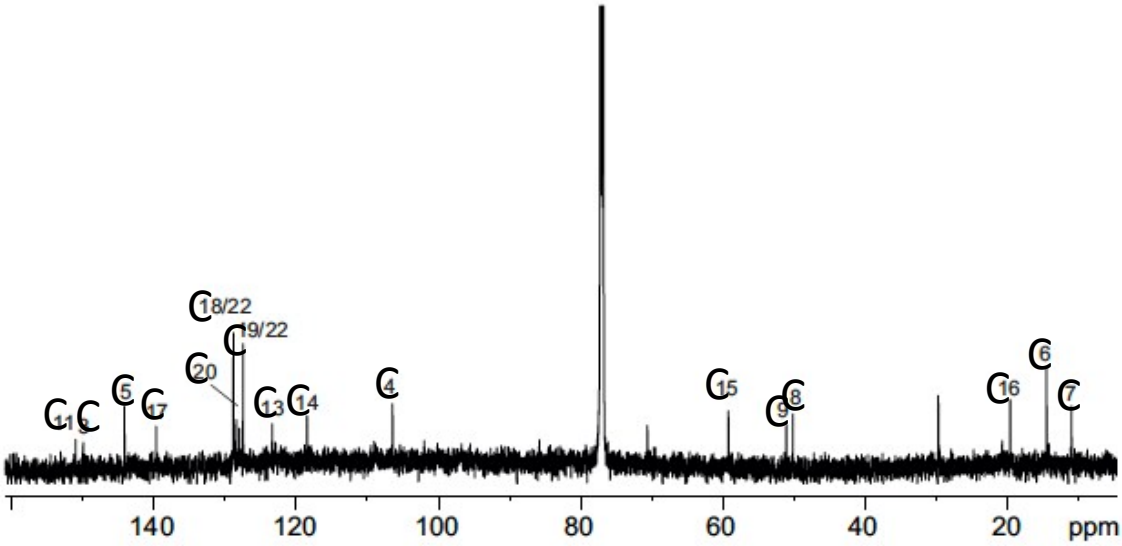
C18/22
C19/22
C20
C5
C17
C11
C12
C13
C14
C4
C15
C9
C8
C16
C6
C7
140
120
100
80
60
40
20
ppm

(c)

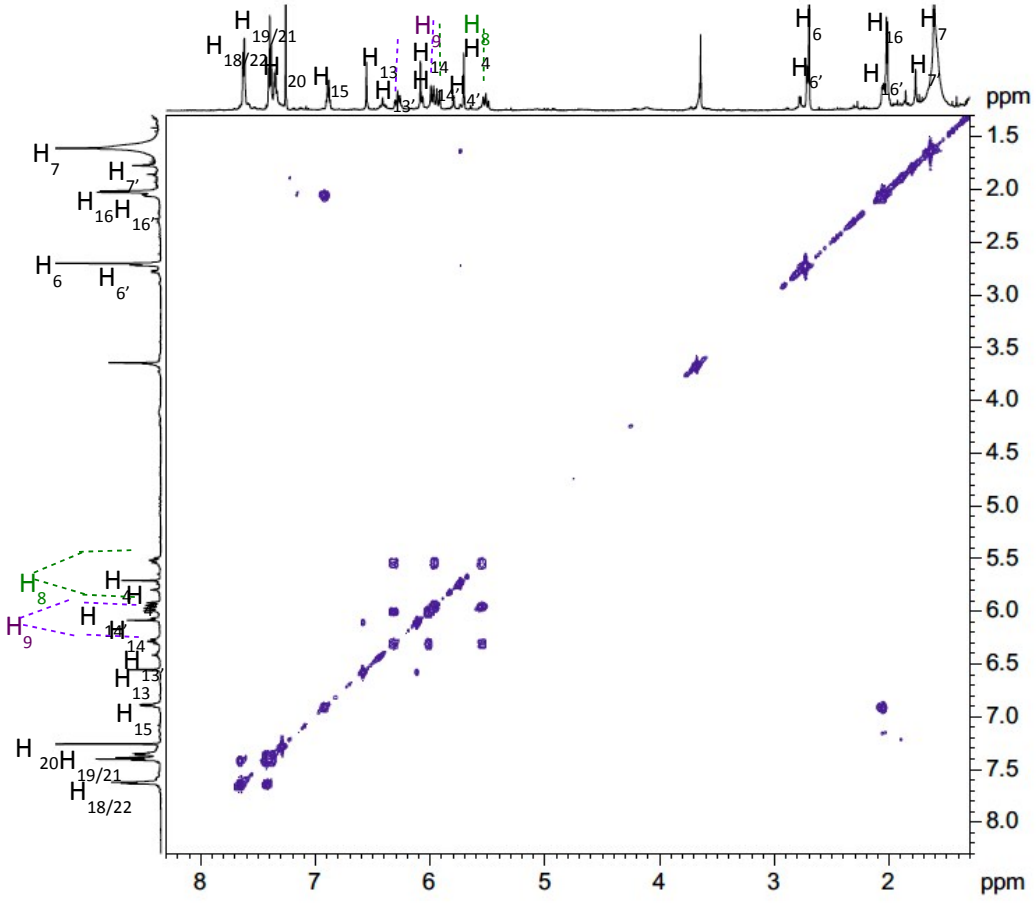
H19/21
H18/22
H20
H15
H13
H13'
H9
H8
H14
H14'
H4
H4'
H6
H6'
H16
H16'
H7
H7'
ppm
1.5
2.0
2.5
3.0
3.5
4.0
4.5
5.0
5.5
6.0
6.5
7.0
7.5
8.0
8
7
6
5
4
3
2
ppm

(d)

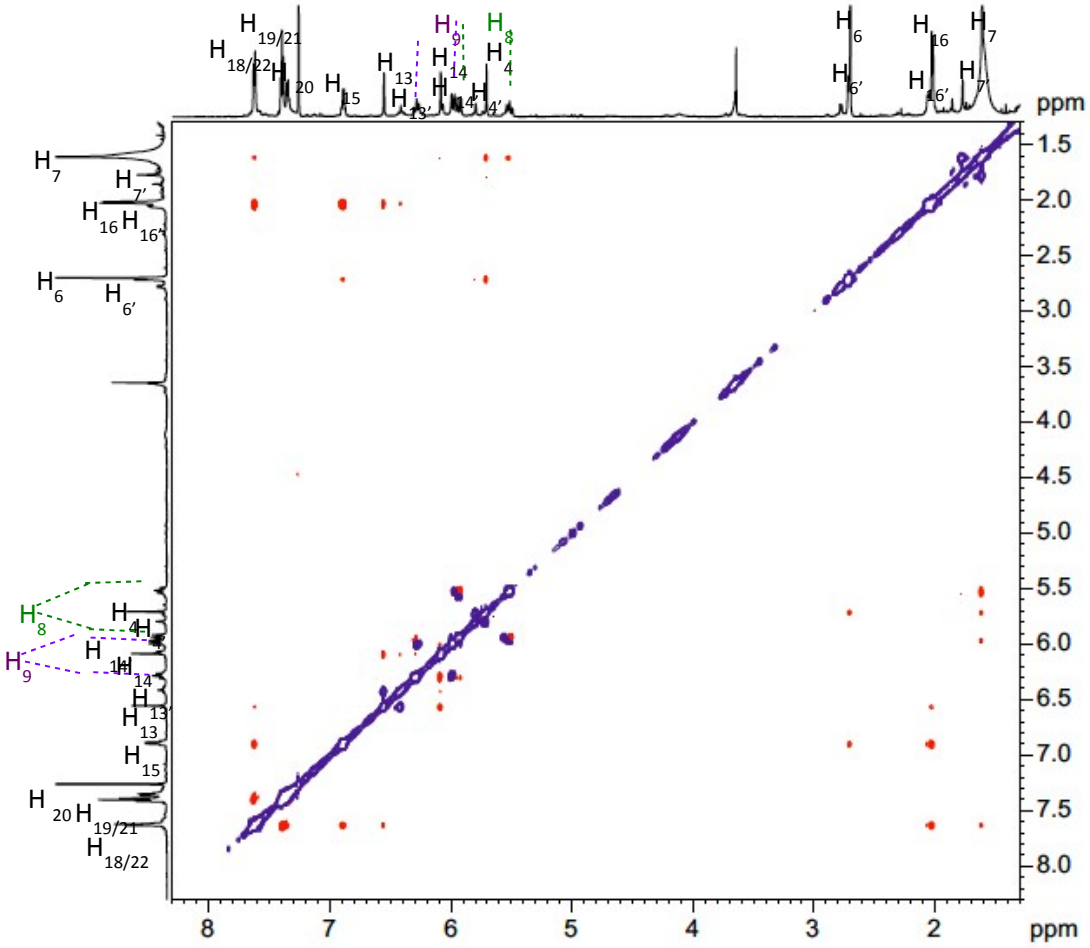
H19/21
H18/22
H20
H15
H13
H13'
H9
H14
H14'
H8
H4
H6
H6'
H16
H16'
H7
H7'
ppm
1.5
2.0
2.5
3.0
3.5
4.0
4.5
5.0
5.5
6.0
6.5
7.0
7.5
8.0
8
7
6
5
4
3
2
ppm

(e)

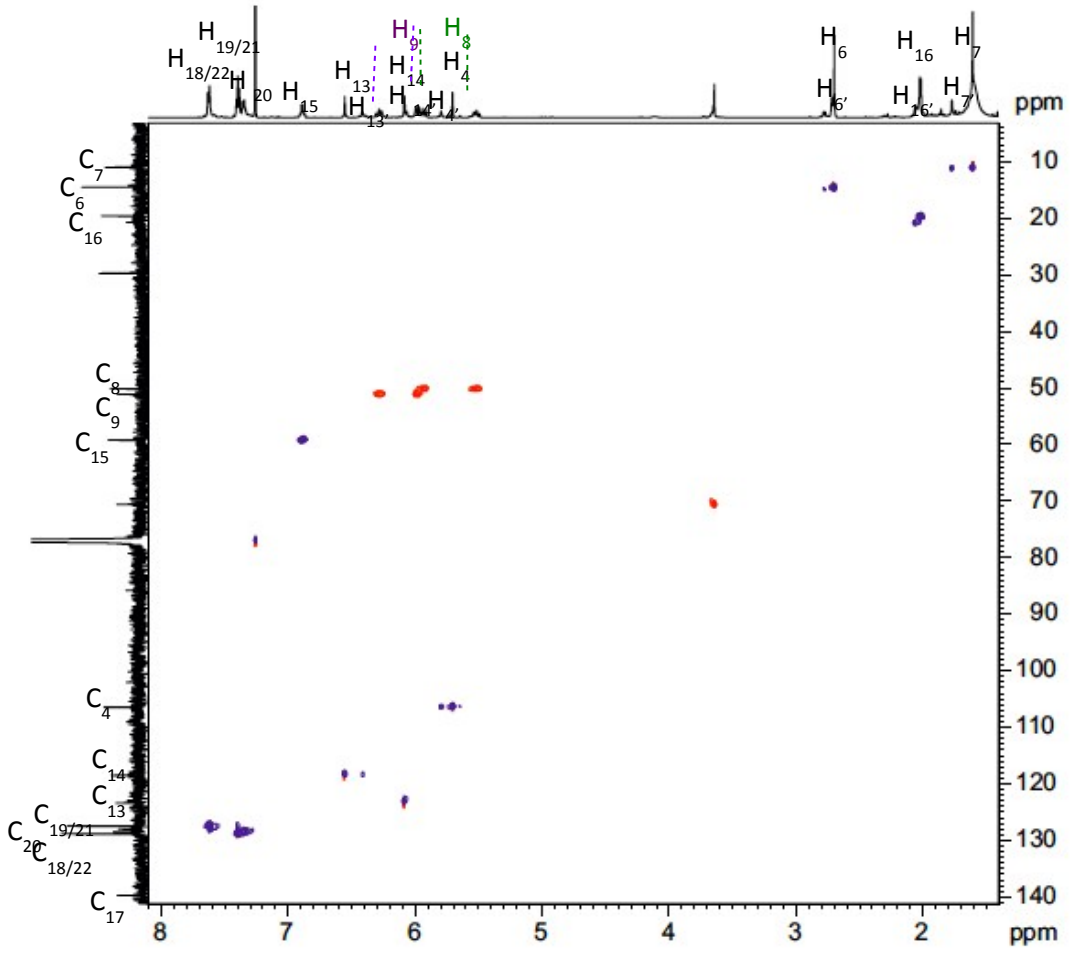
H19/21
H18/22
H20
H15
H13
H9
H14
H8
H4
H6
H16
H7
ppm
C7
C6
C16
C8
C9
C15
C4
C14
C13
C19/21
C20
C18/22
C17
8
7
6
5
4
3
2
ppm

(f)

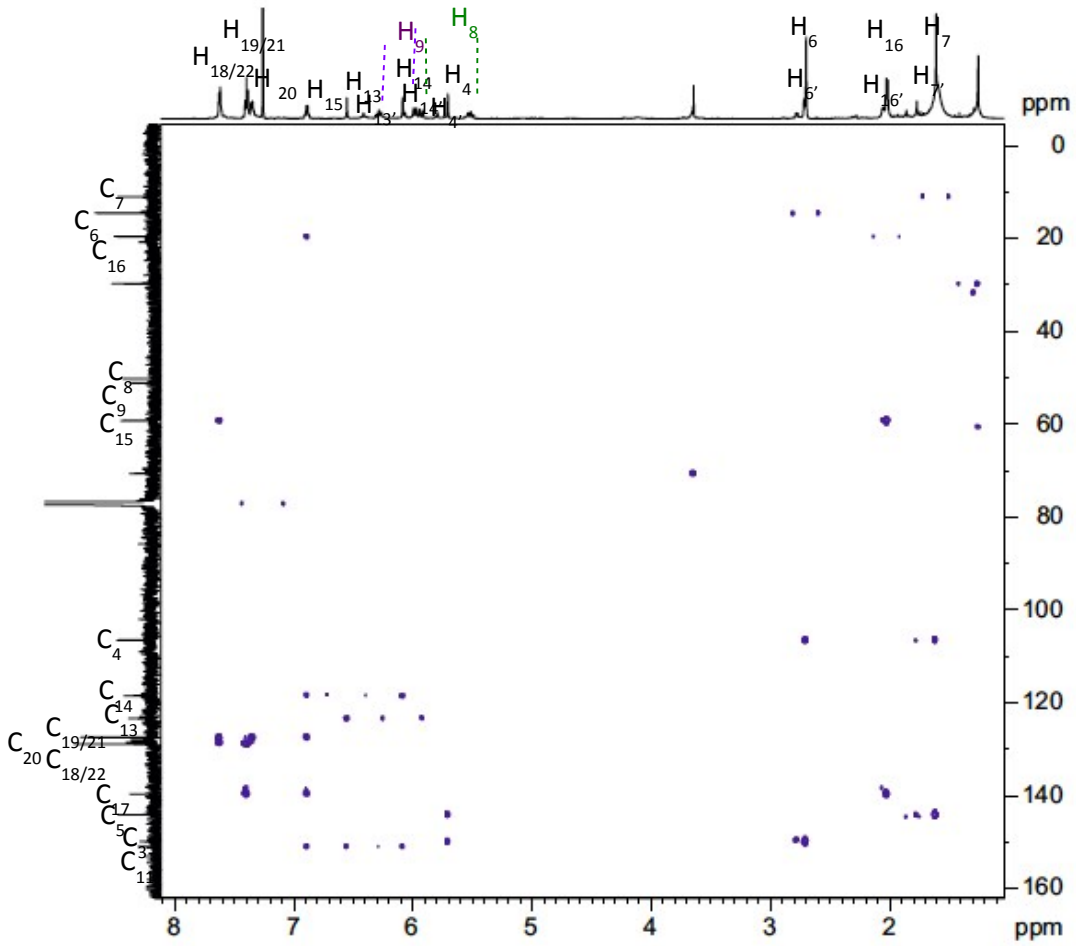
H19/21
H18/22
H20
H15
H13
H13'
H9
H9'
H14
H14'
H8
H4
H4'
H6
H6'
H16
H16'
H7
H7'
ppm
0
20
40
60
80
100
120
140
160
C7
C6
C16
C8
C9
C15
C4
C14
C13
C19/21
C20
C18/22
C17
C5
C3
C11
8
7
6
5
4
3
2
ppm

Figure S13. HR-ESI-MS spectrum of **C1**; (top) experimental, (bottom) simulated.

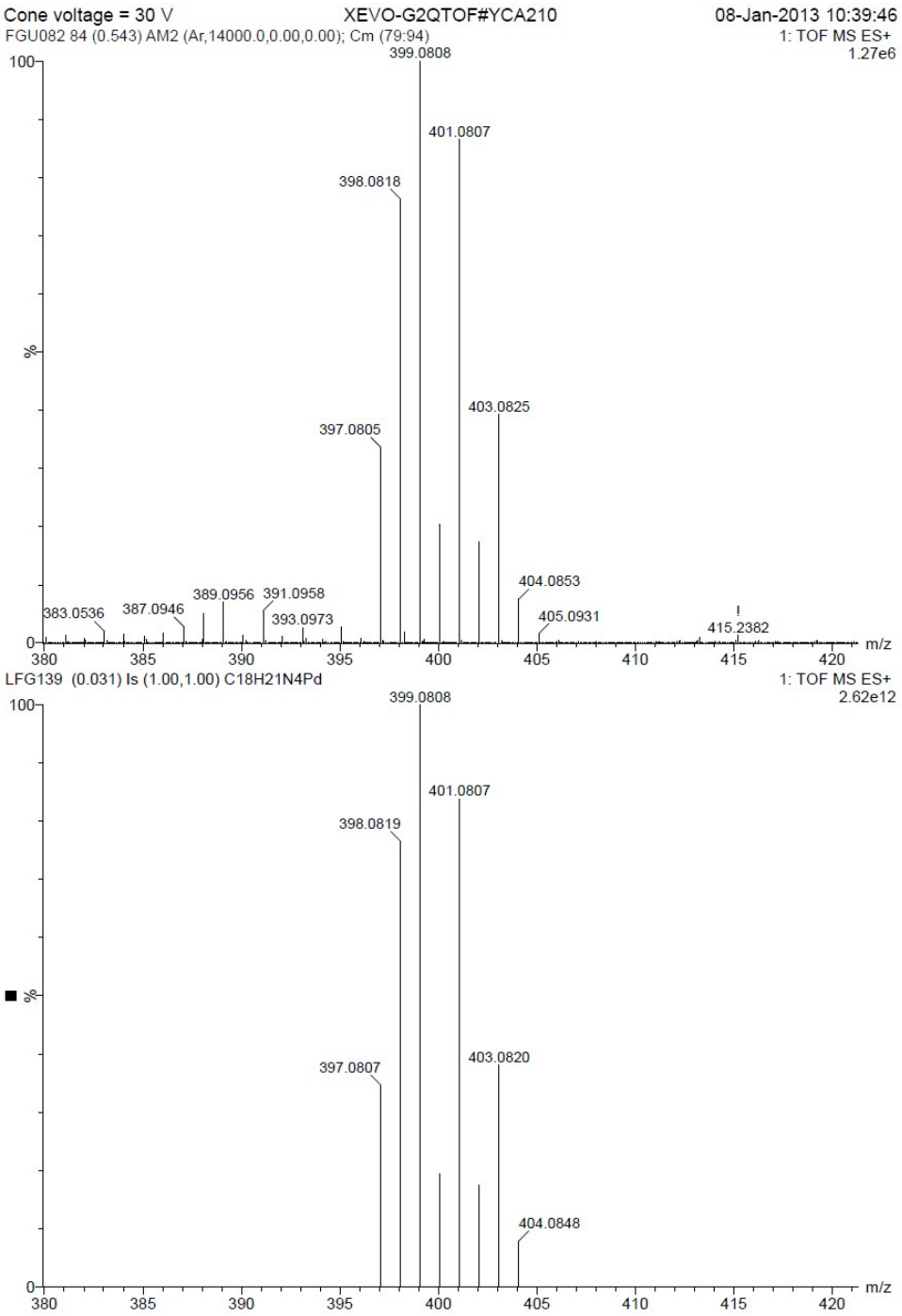

Figure S14. Infrared spectrum of **C1**.

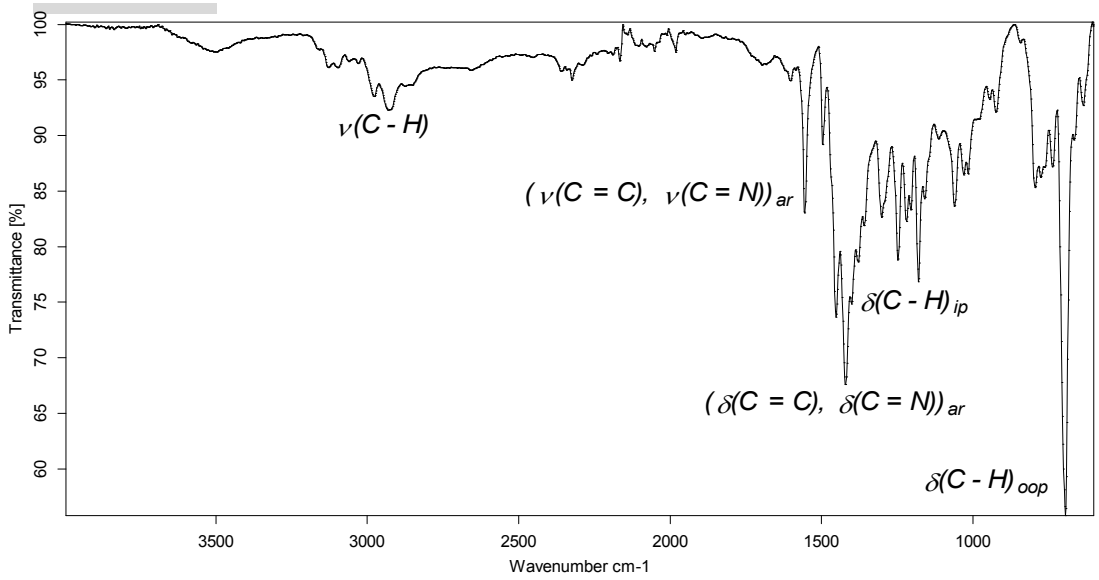

Figure S15. 1D and 2D NMR spectra (360 MHz, 298K, dmso-d_6) for trichloro[(*S*)-3-(2-(3,5-dimethyl-1*H*-pyrazol-1-yl)ethyl)-1-(1-phenylethyl)-1*H*-imidazol-3-ium-κ^1*N*]palladium(II), (**C2**): (a) ^{1}H-NMR, (b) ^{13}C{^{1}H}-NMR, (c) HSQC NMR, (d) COSY NMR.

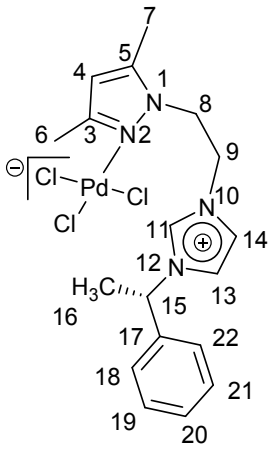

(a)

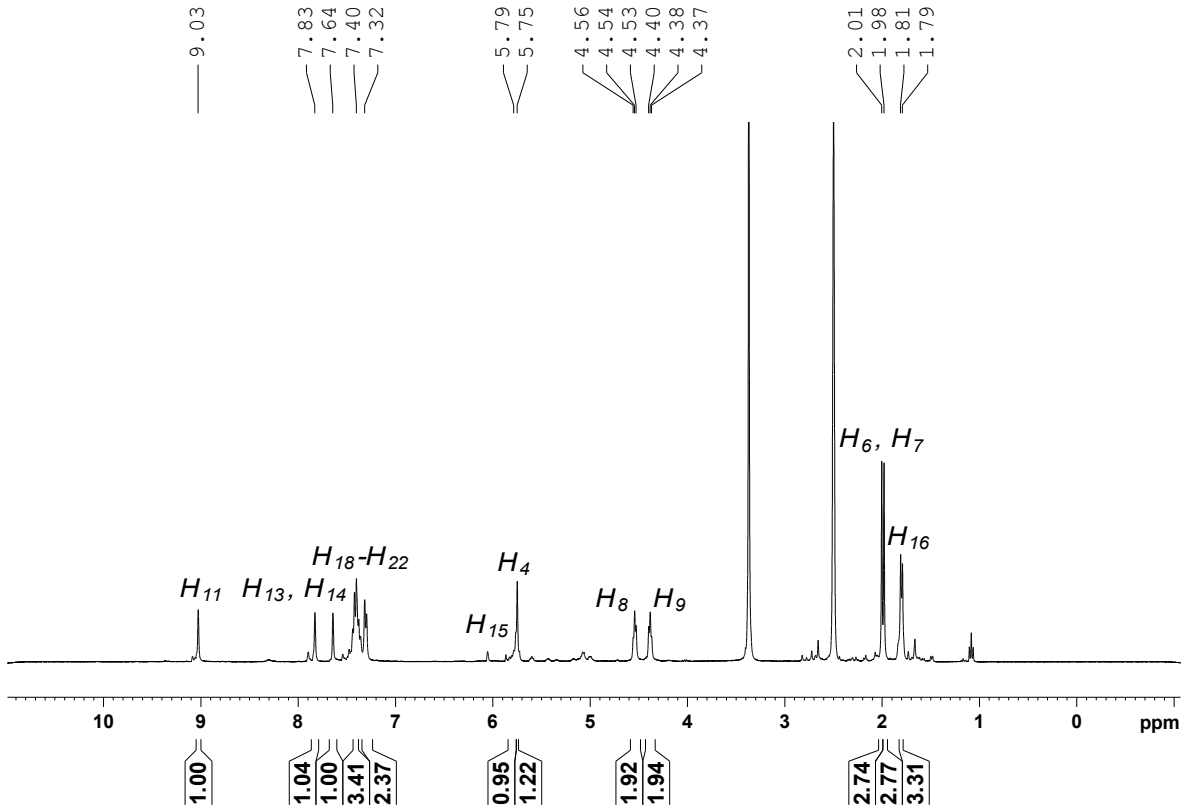

(b)

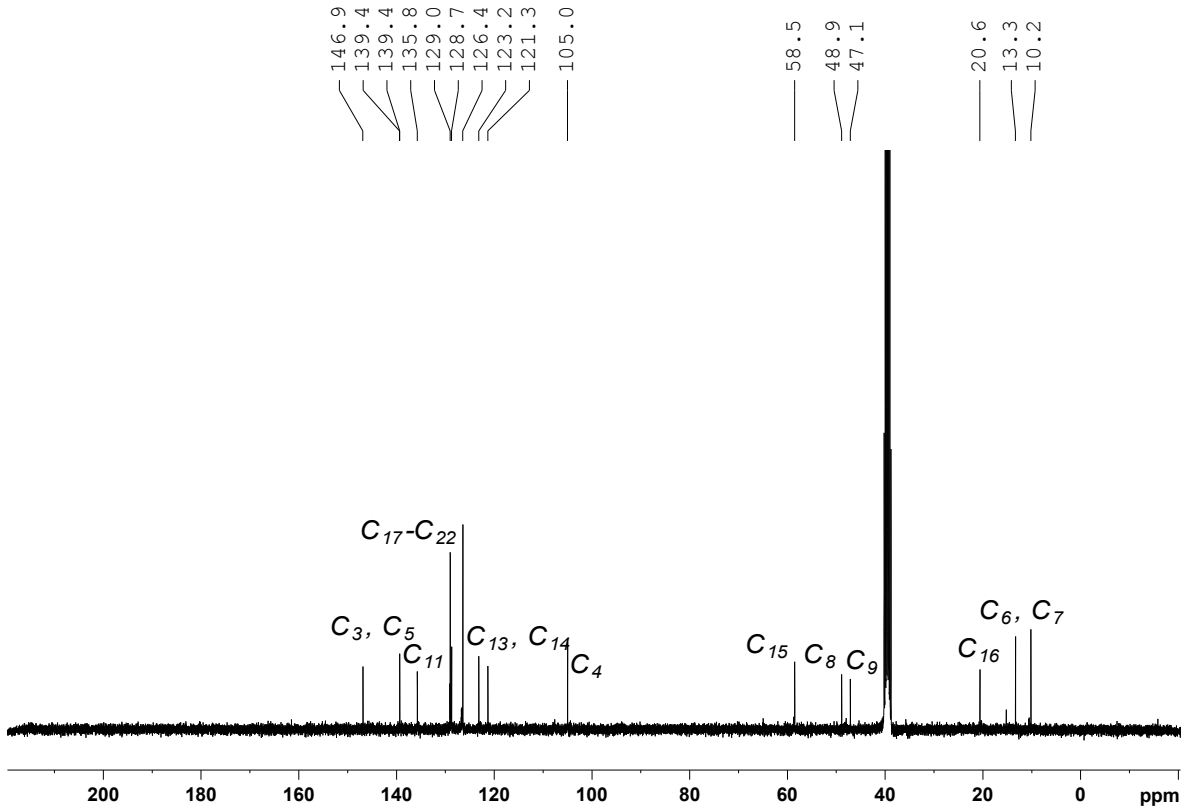
146.9
139.4
139.4
135.8
129.0
128.7
126.4
123.2
121.3
105.0
58.5
48.9
47.1
20.6
13.3
10.2
C17-C22
C3, C5
C11
C13, C14
C4
C15
C8
C9
C16
C6, C7
200
180
160
140
120
100
80
60
40
20
0
ppm

(c)

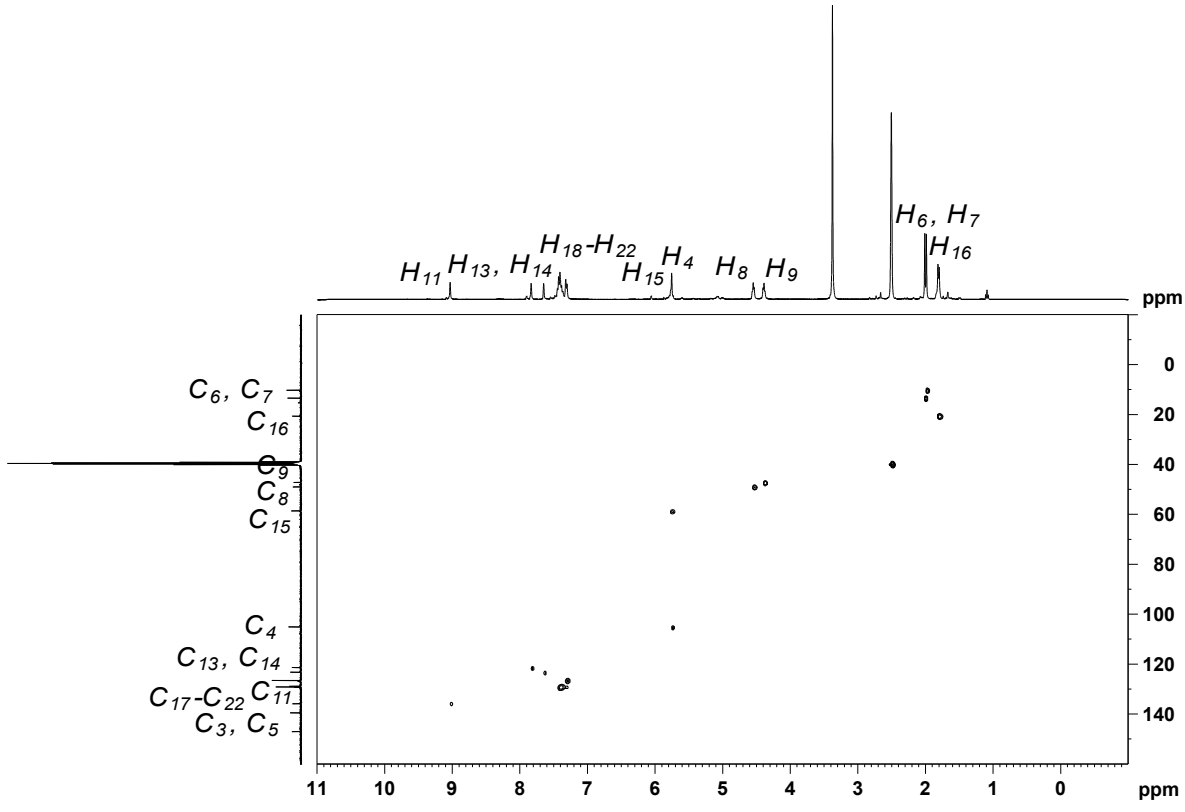
H11
H13, H14
H18-H22
H15
H4
H8
H9
H6, H7
H16
ppm
C6, C7
C16
C9
C8
C15
C4
C13, C14
C17-C22
C11
C3, C5
0
20
40
60
80
100
120
140
11
10
9
8
7
6
5
4
3
2
1
0
ppm

(d)

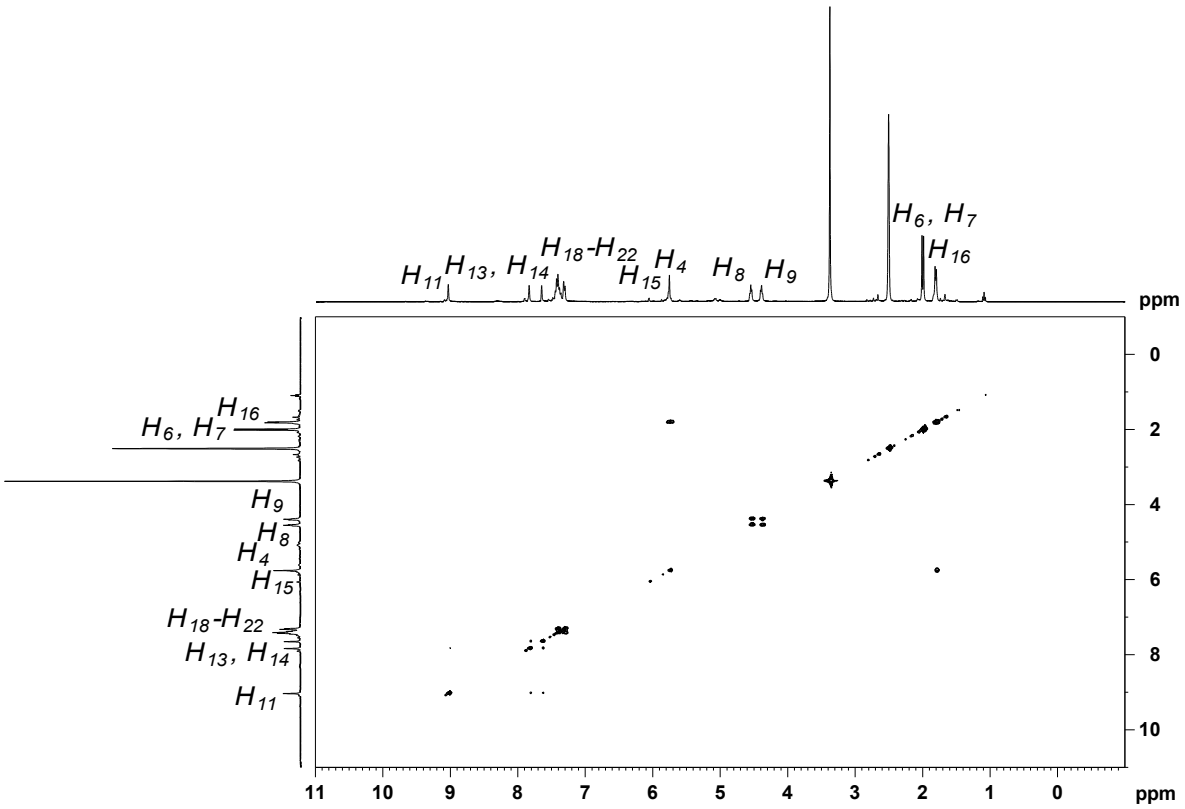

Figure S16. ESI-MS spectrum of **C2**.

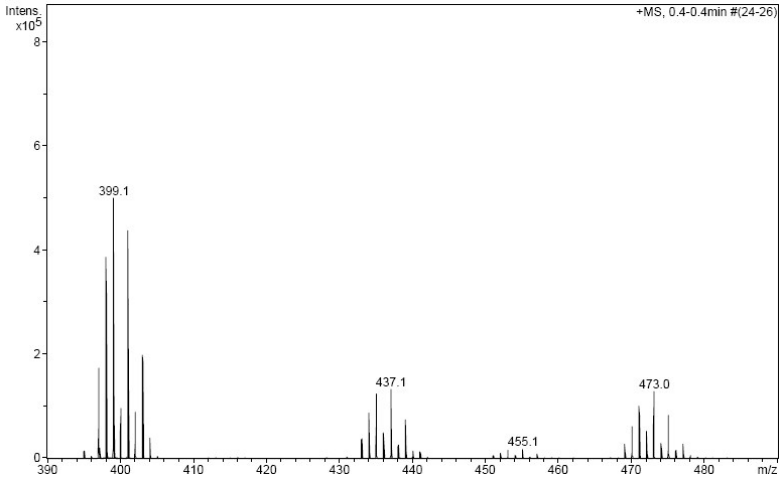

Figure S17. Infrared spectrum of **C2**.

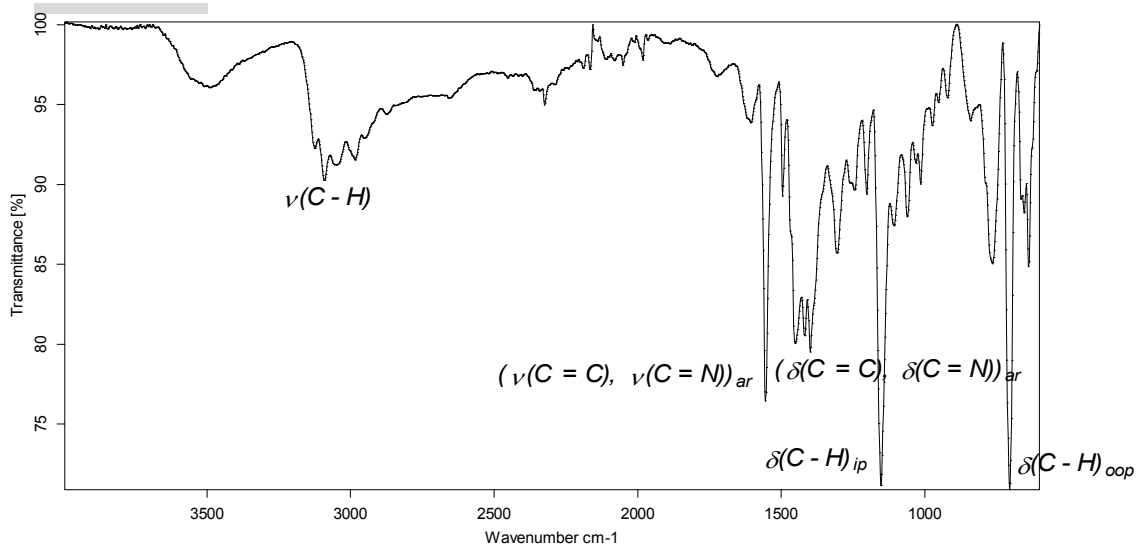

Figure S18. HR-TEM micrographs of Pd nanoparticles (a) **N1** and (b) **N2** after catalytic experiments.

(a)

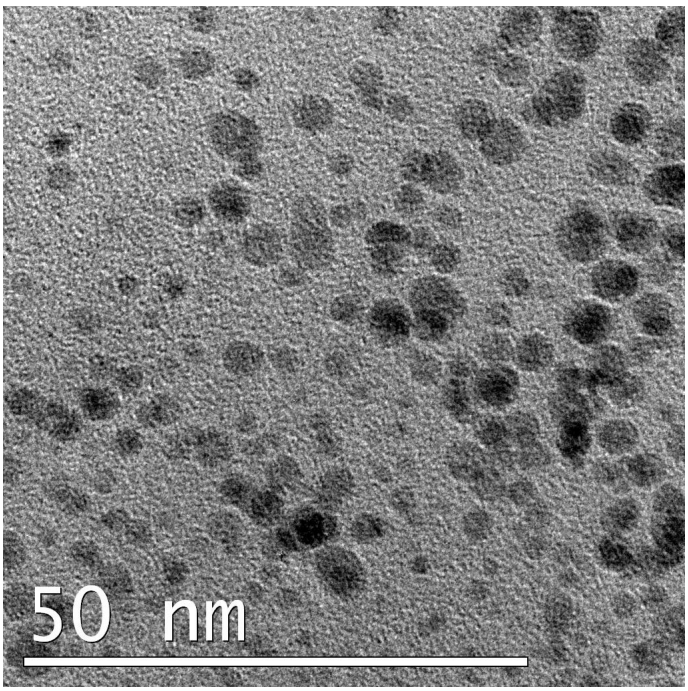

(b)